Title

A Novel Secreted Protein, MYR1, Is Central to Toxoplasma's Manipulation of Host Cells

Journal

mBio, 7(1)

ISSN

2161-2129

Authors

Franco, Magdalena
Panas, Michael W
Marino, Nicole D
et al.

Publication Date

2016-03-02

DOI

10.1128/mbio.02231-15

Peer reviewed

AMERICAN SOCIETY FOR MICROBIOLOGY | mBio®

RESEARCH ARTICLE

A Novel Secreted Protein, MYR1, Is Central to *Toxoplasma*'s Manipulation of Host Cells

Magdalena Franco,[a,b] Michael W. Panas,[a] Nicole D. Marino,[a] Mei-Chong Wendy Lee,[c] Kerry R. Buchholz,[a] Felice D. Kelly,[a] Jeffrey J. Bednarski,[d] Barry P. Sleckman,[e] Nader Pourmand,[c] John C. Boothroyd[a]

Department of Microbiology and Immunology, Stanford University School of Medicine, Stanford, California, USA[a]; Biosciences and Biotechnology Division, Lawrence Livermore National Laboratory, Livermore, California, USA[b]; Department of Biomolecular Engineering, University of California, Santa Cruz, California, USA[c]; Department of Pediatrics, Washington University in St. Louis, St. Louis, Missouri, USA[d]; Department of Pathology and Immunology, Washington University in St. Louis, St. Louis, Missouri, USA[e]

M.F., M.W.P., and N.D.M. contributed equally to this work.

ABSTRACT **The intracellular protozoan *Toxoplasma gondii* dramatically reprograms the transcriptome of host cells it infects, including substantially up-regulating the host oncogene c-*myc*. By applying a flow cytometry-based selection to infected mouse cells expressing green fluorescent protein fused to c-Myc (c-Myc–GFP), we isolated mutant tachyzoites defective in this host c-Myc up-regulation. Whole-genome sequencing of three such mutants led to the identification of *MYR1* (Myc regulation 1; *TGGT1_254470*) as essential for c-Myc induction. MYR1 is a secreted protein that requires TgASP5 to be cleaved into two stable portions, both of which are ultimately found within the parasitophorous vacuole and at the parasitophorous vacuole membrane. Deletion of *MYR1* revealed that in addition to its requirement for c-Myc up-regulation, the MYR1 protein is needed for the ability of *Toxoplasma* tachyzoites to modulate several other important host pathways, including those mediated by the dense granule effectors GRA16 and GRA24. This result, combined with its location at the parasitophorous vacuole membrane, suggested that MYR1 might be a component of the machinery that translocates *Toxoplasma* effectors from the parasitophorous vacuole into the host cytosol. Support for this possibility was obtained by showing that transit of GRA24 to the host nucleus is indeed MYR1-dependent. As predicted by this pleiotropic phenotype, parasites deficient in *MYR1* were found to be severely attenuated in a mouse model of infection. We conclude, therefore, that MYR1 is a novel protein that plays a critical role in how *Toxoplasma* delivers effector proteins to the infected host cell and that this is crucial to virulence.**

IMPORTANCE ***Toxoplasma gondii* is an important human pathogen and a model for the study of intracellular parasitism. Infection of the host cell with *Toxoplasma* tachyzoites involves the introduction of protein effectors, including many that are initially secreted into the parasitophorous vacuole but must ultimately translocate to the host cell cytosol to function. The work reported here identified a novel protein that is required for this translocation. These results give new insight into a very unusual cell biology process as well as providing a potential handle on a pathway that is necessary for virulence and, therefore, a new potential target for chemotherapy.**

Received 23 December 2015 **Accepted** 5 January 2016 **Published** 2 February 2016

Citation Franco M, Panas MW, Marino ND, Lee M-CW, Buchholz KR, Kelly FD, Bednarski JJ, Sleckman BP, Pourmand N, Boothroyd JC. 2016. A novel secreted protein, MYR1, is central to *Toxoplasma*'s manipulation of host cells. mBio 7(1):e02231-15. doi:10.1128/mBio.02231-15.

Editor Arturo Casadevall, Johns Hopkins Bloomberg School of Public Health

Address correspondence to John C. Boothroyd, jboothr@stanford.edu.

Toxoplasma gondii is an obligate intracellular parasite of great medical importance, as infections in immunosuppressed patients often lead to life-threatening encephalitis. While *Toxoplasma* bradyzoites localize to specific tissues (brain, skeletal muscles, and heart) (1) during the chronic phase, the acute stages of infection involve tachyzoites that are able to infect virtually any nucleated cell. *Toxoplasma*'s intracellular lifestyle is dependent on the ability of the parasite to regulate host cell processes via its secreted effectors. For example, the rhoptry protein ROP16 regulates the immunologically important host transcription factors STAT1 (2), STAT3 (3), STAT5 (4), and STAT6 (5), causing profound transcriptional changes shortly after invasion. Further examples of *Toxoplasma*'s ability to specifically regulate host functions are its dense granule effectors GRA15 (6), GRA16 (7), and GRA24 (8), which regulate the NF-κB, p53, and p38 MAP kinase (MAPK) host pathways, respectively.

We have recently discovered that *Toxoplasma* tachyzoites also specifically and actively induce host c-Myc upon infection (9). c-Myc is a key transcription factor that regulates critical host cell processes such as cell cycle progression, cell metabolism, and apoptosis (10, 11), and several of these c-Myc-regulated processes appear to be modulated in *Toxoplasma*-infected cells (12). In addition, and likely as a direct consequence of its up-regulation, many of the known gene targets of c-Myc have also been reported to be transcriptionally up-regulated during *Toxoplasma* infection (9). The up-regulation of c-Myc is likely mediated by one or more novel effectors, since none of the previously identified *Toxoplasma* effectors appear to play a role (7, 9).

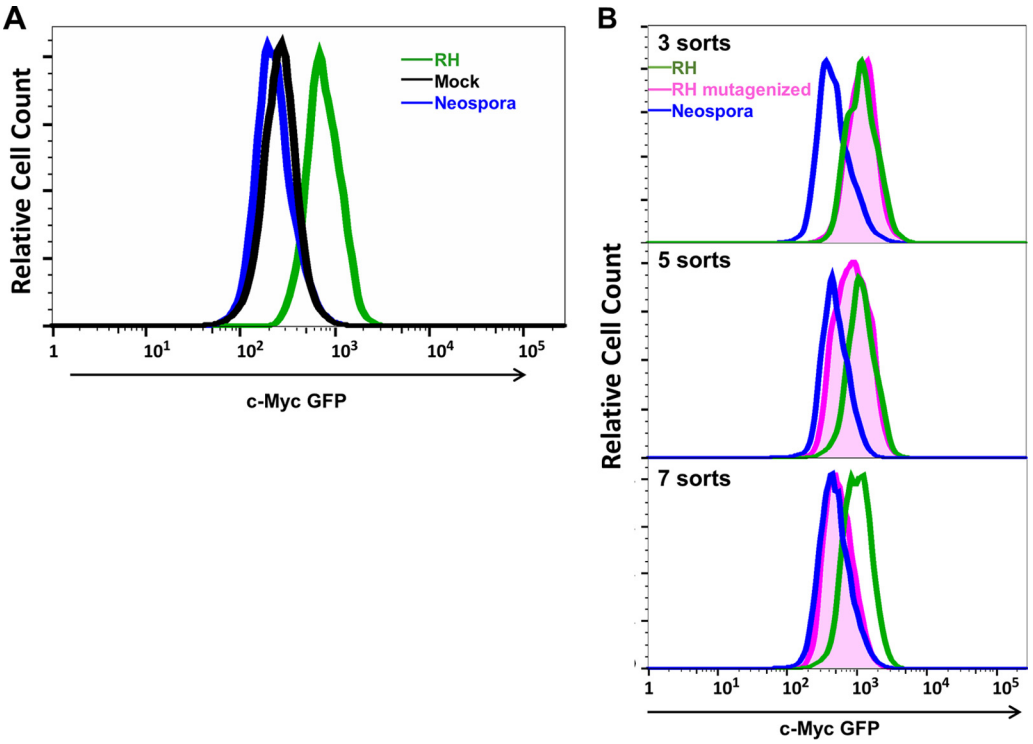

FIG 1 Genetic screen to isolate *Toxoplasma* mutants that fail to induce c-Myc. (A) Flow cytometry histogram of BMMs expressing c-Myc–GFP infected with *Toxoplasma* wild-type tachyzoites (RH) or *Neospora* tachyzoites or mock-infected. The gate was set on highly infected cells. The *y* axis shows relative cell count for each population (normalized to mode), and the *x* axis shows green fluorescence intensity. (B) Selection of mutants that fail to induce c-Myc. BMM c-Myc–GFP reporter cells were infected with a mutagenized population of RH tachyzoites and sorted for low GFP fluorescence. This was repeated until a homogeneous population was obtained that induced low GFP fluorescence. The GFP fluorescence profiles for the mutagenized population after 3, 5, and 7 rounds of selection are shown. (Histograms for first two sorts were similar to the one for sort 3 and were omitted.) The profiles for cells infected with wild-type RH and *Neospora* tachyzoites are shown for comparison. The *x* and *y* axes are as described for panel A.

The mechanism by which secreted effectors reach the host cytosol in *Toxoplasma*-infected cells is not known. In the related malaria parasites *Plasmodium* spp., proteins are translocated across the parasitophorous vacuole membrane (PVM) via the PTEX complex (13–15). *Toxoplasma* has recognizable orthologues of some components of this complex, but recent reports show that these operate in different ways; e.g., the *Toxoplasma* orthologue of EXP2 is GRA17, but recent work showed that this protein serves as a transporter of small molecules (<3,000 Da), not proteins (16).

To further explore the process by which *Toxoplasma* effectors operate, we chose a genetic approach that exploits the fact that *Toxoplasma* tachyzoites up-regulate c-Myc and the existence of faithful c-Myc reporter systems. Here we describe the use of such a screen to identify mutants deficient in a novel *Toxoplasma* protein that is secreted into the parasitophorous vacuole (PV) and is necessary for host c-Myc induction. We show that mutations in this gene, which we have dubbed *MYR1* (Myc regulation 1), are pleiotropic with a pronounced defect in the ability of tachyzoites to manipulate several host pathways, and we propose a role for MYR1 in protein translocation across the PVM.

RESULTS

Isolation of *Toxoplasma* mutants that fail to induce c-Myc. Forward genetic screens have previously identified important *Toxoplasma* proteins involved in various functions (17–20). Such an approach is facilitated by the fact that the *Toxoplasma* genome is haploid, and thus, single mutations often give rise to discrete phenotypes. To further investigate how *Toxoplasma* tachyzoites interact with the host cell, therefore, we designed a high-throughput genetic screen to isolate mutants defective in their ability to modulate a known and easily studied pathway, the up-regulation of c-Myc. The major requirement for such a screen is a reporter cell that allows easy detection of c-Myc expression levels. For this, we first attempted several plasmid-based systems involving the c-Myc promoter driving reporters such as GFP in established cell lines; unfortunately, however, none showed up-regulation upon infection with *Toxoplasma* tachyzoites (data not shown). This suggested that the up-regulation required c-*myc* to be in its natural chromosomal location, where it is known to be regulated by a complex array of enhancers, including at least one that is >400 kbp distant (21).

To overcome the limitation of plasmid-based reporters, we examined bone marrow macrophages (BMMs) from mice engineered to express green fluorescent protein (GFP) fused to the N terminus of c-Myc and expressed from the native c-*myc* locus (22). BMMs were isolated from the mice and infected at a multiplicity of infection (MOI) of 0.25 with either *Toxoplasma* RH mCherry or *Neospora caninum* NC-1 mCherry (9) or were mock-infected. Approximately 24 h postinfection (hpi), flow cytometry was used to distinguish between infected (mCherry-positive) and uninfected (mCherry-negative) cells and to analyze GFP levels in

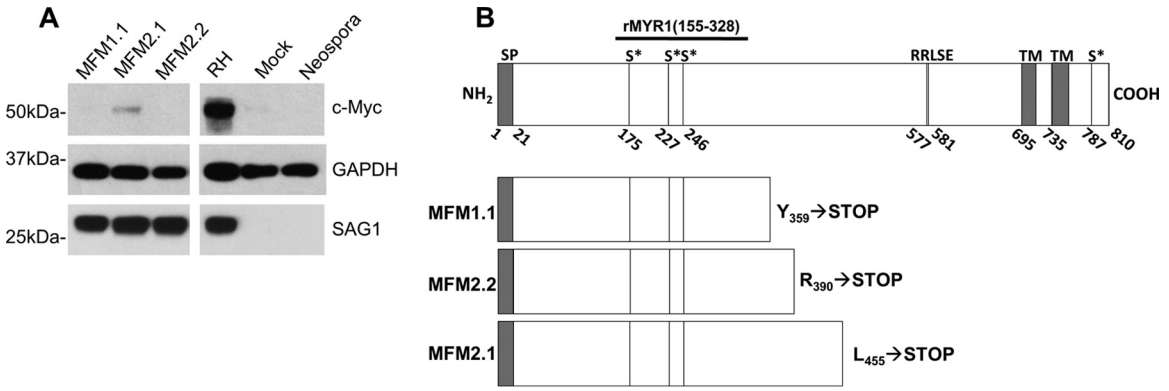

FIG 2 Characterization of *Toxoplasma* mutants that fail to up-regulate c-Myc in host cells. (A) Human foreskin fibroblasts (HFFs) were infected with wild-type parasites (RH) or mutant strains MFM1.1, MFM2.1, and MFM2.2. *Neospora*- and mock-infected fibroblasts were used as negative controls for c-Myc induction. Lysates from infected cells were prepared at 20 hpi, and host c-Myc levels were analyzed by Western blotting using anti-human c-Myc antibodies. Anti-hGAPDH staining was used as a loading control for host (human) protein, and anti-SAG1 staining was used to show comparable levels of *Toxoplasma* infection. Each row is derived from the same exposure of the same blot; the white vertical separator shows where irrelevant data were removed from the image. (B) Schematic diagram of wild-type and mutant TGGT1_254470 (MYR1) protein. Numbers indicate amino acid positions relative to the predicted N terminus of the unprocessed protein. The signal peptide (SP) is as predicted by the SignalP 4.1 tool (http://www.cbs.dtu.dk/services/SignalP/) and ToxoDB (http://www.toxodb.org) and phosphorylated serine (S*) residues were determined by phosphoproteomic analysis (24). The region expressed as a recombinant version of MYR1 representing amino acids 155 to 328 to generate an N-terminus-specific antibody is indicated by the solid line [rMYR1(155–328)]. Transmembrane domains are as predicted by the TMHMM algorithm and ToxoDB (http://www.cbs.dtu.dk/services/TMHMM-2.0/), and the position of the first residue of each is indicated. A likely ASP5 cleavage site (RRLSE) is as described in the text. Mutant versions of MYR1, as predicted by sequencing strains MFM1.1, MFM2.1, and MFM2.2, are also shown. The letters and numbers to the right of each schematic show the original coding function and position of the nonsense mutation in each.

both populations (Fig. 1A). The results showed that, compared to mock-infected reporter cells, *Toxoplasma*-infected cells exhibited a marked increase in green fluorescence. Infection with *Neospora* showed no c-Myc up-regulation, as previously reported (9).

Having identified a reporter system that recapitulates the *Toxoplasma*-induced up-regulation of c-Myc, we next designed a genetic screen for *Toxoplasma* mutants that are deficient in this process. Mutagenized *Toxoplasma* RH parasites expressing mCherry were used to infect the c-Myc–GFP reporter BMMs at an MOI of 0.25. A low multiplicity of infection was used to ensure that most reporter cells were infected with only one parasite, which was confirmed visually by fluorescence microscopy. *Toxoplasma* wild-type-infected cells and mock-infected cells were used as positive and negative controls for c-Myc induction, respectively. Cells with high levels of red fluorescence but little or no GFP signal were then selected by fluorescence-activated cell sorting (FACS). *Neospora*-infected cells were used to establish selection gates for the enrichment of mutants. Parasites in the selected cells, representing between 1 and 5% of the total infected population, were expanded by growth in human foreskin fibroblasts (HFFs), and selection in c-Myc-reporter BMMs was repeated a further seven times. A phenotypically distinct population began to emerge after 5 enrichments, and after a further 2 rounds of selection, the mutant phenotype (failure to induce c-Myc–GFP) was uniformly present in the entire population (Fig. 1B). This population was dubbed MFM1 (Magdalena Franco c-Myc mutant population 1), and parasite clones derived from this population were sequentially numbered MFM1.1, MFM1.2, etc.

To obtain independent mutants for the purposes of whole-genome sequencing analysis, the screen was repeated with an independently mutagenized population of *Toxoplasma* parasites. This time, more stringent gates were used during selection of the mutant parasites (selecting for the lowest 1% of infected cells in terms of green fluorescence), and only 5 rounds of selection were necessary to isolate parasites deficient in c-Myc induction (data not shown). This population was dubbed MFM2 and was subjected to limiting dilution to yield the putative clones, MFM2.1, MFM2.2, etc.

To verify that the isolated *Toxoplasma* mutant strains are indeed deficient in c-Myc up-regulation, c-Myc levels in lysates prepared from HFFs infected with each of three mutant lines, MFM1.1, MFM2.1, and MFM2.2, representing the two independently generated mutant pools, were analyzed by Western blotting. Mock-infected and *Neospora*-infected cells served as negative controls for c-Myc induction, and cells infected with wild-type *Toxoplasma* were used as a positive control. The results (Fig. 2A) showed that cells infected with two of the three cloned mutants, MFM1.1 and MFM2.2, showed no detectable c-Myc, indicating the selection strategy was successful in yielding *Toxoplasma* mutants deficient in c-Myc up-regulation. MFM2.1 had an intermediate phenotype, which is discussed further below.

Whole-genome sequence analysis reveals a candidate gene, *TGGT1_254470*. To identify the *Toxoplasma* gene(s) involved in c-Myc up-regulation, the MFM1.1, MFM2.1, and MFM2.2 mutants were analyzed by whole-genome sequencing. Sequence comparison relative to the parental reference revealed 5, 7, and 6 single nucleotide variations (SNVs), respectively, in chromosomal coding regions of MFM1.1, MFM2.1, and MFM2.2 (Table 1). These results showed that although they came from the same screen, MFM2.1 and MFM2.2 are independent mutants, as each contained a different set of SNVs. The independence of MFM1.1, which was isolated from the first screen, was also confirmed by the sequencing. MFM2.1 had no SNVs with a read frequency over 80% but several within the ~40-to-60% range (Table 1). This indicates that the sample containing MFM2.1 is in fact a mix of two

TABLE 1 Coding mutations in mutant strains as detected by whole-genome sequencing[a]

Clone and chromosome	SNV position	% confidence	Codon (WT/mut)[b]	Amino acid change[c]	Gene	Predicted function
MFM1.1						
TGGT1_chrX	6416305	97	tgC/tgG	C1296W	TGGT1_214830	Hypothetical protein
TGGT1_chrVIII	1852637	100	caT/caA	H643Q	TGGT1_232100	RAP domain-containing protein
TGGT1_chrVIII	216920	100	gAa/gGa	E135G	TGGT1_229380	Hypothetical protein
TGGT1_chrXII	3209479	100	gTc/gGc	V125G	TGGT1_247350	Thioredoxin domain-containing protein
TGGT1_chrIII	1740887	100	taT/taA	Y281*	TGGT1_254470	Hypothetical protein
MFM2.1						
TGGT1_chrVIIb	3288737	42	tCa/tTa	S151L	TGGT1_258580	Rhoptry protein ROP17
TGGT1_chrIX	2870406	42	Aaa/Gaa	K526E	TGGT1_289190	Tetratricopeptide repeat-containing protein
TGGT1_chrXI	3283667	43	gGa/gAa	G635E	TGGT1_313370	Hypothetical protein
TGGT1_chrVI	583819	46	gaG/gaT	E294D	TGGT1_239365	Formyl transferase domain-containing protein
TGGT1_chrX	4899763	46	Acc/Ccc	T781P	TGGT1_235640	Formyl transferase domain-containing protein
TGGT1_chrVIIa	3223402	56	aTt/aCt	I53T	TGGT1_202445	Hypothetical protein
TGGT1_chrIII	1741174	41	tTa/tGa	L377*	TGGT1_254470	Hypothetical protein
MFM 2.2						
TGGT1_chrV	989081	100	Ggc/Agc	G51S	TGGT1_213520	Peptidase M20D, amidohydrolase
TGGT1_chrVIII	4035211	100	Tat/Cat	Y170H	TGGT1_272370	Hypothetical protein
TGGT1_chrX	6416305	100	tgC/tgG	C1296W	TGGT1_214830	Hypothetical protein
TGGT1_chrXII	6308563	100	Aag/Gag	K2346E	TGGT1_277940	Hypothetical protein
TGGT1_chrXII	1807927	100	Tca/Aca	S601T	TGGT1_217480	Hypothetical protein
TGGT1_chrIII	1740978	100	Cga/Tga	R312*	TGGT1_254470	Hypothetical protein

[a] The position and nature of all coding SNVs in chromosomal genes in each mutant are listed. Only mutations that were supported by at least 80% of the reads in MFM1.1 and MFM2.2 or 40% of the reads in MFM2.1 were considered SNVs.
[b] WT, wild type; mut, mutant. Capital letters indicate the mutated nucleotides.
[c] *, Stop codon.

lines, consistent with its intermediate phenotype in terms of c-Myc up-regulation, as shown in Fig. 2A.

In addition to the SNVs in chromosomal genes shown in Table 1, mutations might also be present in genes present on relatively short contigs that have yet to be confidently positioned on any chromosome, likely because they are tandemly duplicated genes that are difficult to unambiguously assemble. Identifying mutations in the latter set is particularly challenging because the short sequence reads often cannot be unambiguously assigned to one or other of the tandemly repeated genes and a false assignment may erroneously be taken as an SNV. We did not attempt to resolve SNVs in such contigs and it is possible, therefore, that additional coding SNVs, beyond those shown in Table 1, exist within the mutants.

Of all the identified SNVs, only one *Toxoplasma* gene (designated *TGGT1_254470* in ToxoDB v.10.0; http://www.toxodb.org) carried an alteration in two or more mutants; in fact, it was altered in all three mutants (Table 1), each of which carried a nonsense mutation at a different position (Fig. 2B). Moreover, *TGGT1_254470* was the only gene to harbor a nonsense mutation in any of the three mutants (Table 1). These data strongly suggested that *TGGT1_254470* is necessary for c-Myc induction in *Toxoplasma*-infected host cells, and it was therefore dubbed *MYR1* for its essential role in c-Myc regulation.

MYR1 is located on chromosome III and is predicted by ToxoDB (v25) to have 4 or 5 introns, depending on the strain. Aggregate RNA-Seq data in ToxoDB, however, clearly show that in most strains, the extra intron predicted in TgME49_254470 (positions 1758697 to 1759101) is rarely, if ever, spliced out, and this region is instead fully represented in the bulk of the final mRNA generated. This impacts the predicted open reading frame and extends it 234 bp in the 5′ direction, relative to what is shown for TgME49_254470, resulting in a different predicted start codon (position 1758990, as we have now noted in the comment section for this gene in ToxoDB). Use of this upstream start codon results in the presence of a strongly predicted signal peptide by SignalP 4.1 with a discrimination score (*D* score) of 0.77, where any score above 0.45 is judged significant. This is consistent with the fact that the MYR1 protein is secreted from the parasite (see below). We conclude, therefore, that the extra intron predicted for *MYR1* is typically not spliced out and that the true start site for translation is at nucleotide 1758990.

Expressed sequence tag data, microarray data, and RNA-Seq data, also available on ToxoDB (v25), show that this gene is abundantly expressed across the three major infectious stages of *Toxoplasma*, tachyzoites, bradyzoites, and sporozoites but is expressed little if at all (<5% of the RPKM [reads per kilobase per million] values for tachyzoites) in the intraepithelial stages in the cat gut (23–27). Its function, therefore, may not be key to the sexual cycle of the parasite that occurs exclusively in felines.

Multiple sequence alignment of nucleotide and protein sequences using the Clustal Omega alignment tool on EMBL-EBI website (http://www.ebi.ac.uk) revealed that this protein is highly conserved (>99% identity) among the three canonical strains, RH (type I), ME49 (type II), and VEG (type III). Likewise, it is expressed at similar levels in tachyzoites from these three strains (ToxoDB [v25]). These similarities were as expected given that all three major types exhibit the c-Myc induction phenotype (9).

MYR1 encodes a novel protein with two predicted transmembrane domains located near its C terminus (Fig. 2B). PsiBLAST analysis of the entire protein sequence revealed no predicted function and no homology to proteins outside its closest relatives,

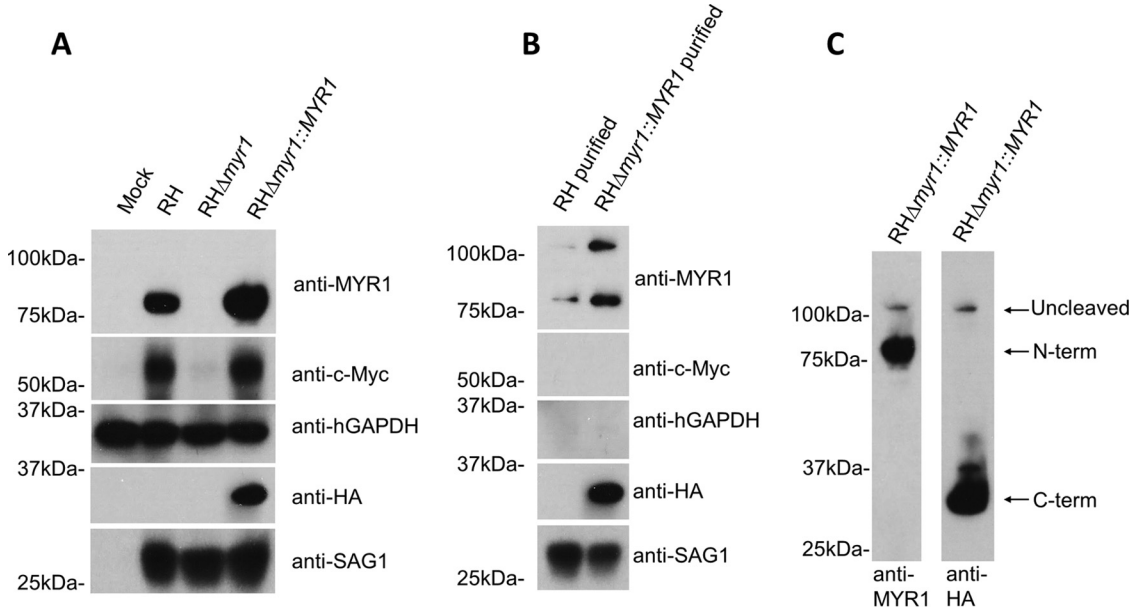

FIG 3 MYR1 is a secreted protein that is necessary for c-Myc induction. (A) HFFs were infected at an MOI of 1 with the indicated strain and lysed at 20 hpi, and lysates were analyzed by Western blotting using anti-MYR1 antibodies and anti-HA antibodies to detect endogenous and recombinant MYR1 levels. Rabbit anti-c-Myc antibodies were used to assess the levels of c-Myc in each sample. Anti-GAPDH and anti-SAG1 antibodies served as loading controls for cells and parasites, respectively. (B) As described for panel A, except the monolayers were scrape-syringed and tachyzoites were purified away from host cell material prior to the lysate being prepared. An additional band at ~105 kDa is apparent in these lysates. (C) Anti-MYR1 and anti-HA blots of cell lysate prepared from HFFs infected with complemented (RHΔ*myr1*::*MYR1*) parasites. These blots were overexposed so the slow-running band (~105 kDa) corresponding to full-length MYR1 and detected by both antibodies can be seen.

Hammondia hammondi and *Neospora caninum*. The orthologue of *MYR1* present in the very closely related *H. hammondi* (*HHA_254470*) is 87% identical at the amino acid level, as expected, but in *N. caninum* (*NCLIV_008760*), there is only ~45% predicted protein identity relative to the *Toxoplasma* (GT1) protein (ToxoDB v25). No convincing homologue is detectable in *Sarcocystis neurona* or the more distantly related apicomplexan genera *Eimeria* and *Plasmodium*. These results suggest a function specific to a subset of the tissue-dwelling coccidia.

MYR1 is necessary for host c-Myc induction. To confirm that MYR1 is involved in the c-Myc induction phenotype, we generated a targeted deletion of the *MYR1* locus in RH type I *Toxoplasma* and produced a complemented version of this Δ*myr1* strain in which a C-terminally hemagglutinin (HA)-tagged version of the *MYR1* gene is ectopically expressed in the knockout (RHΔ*myr1*::*MYR1*; see Materials and Methods). Successful deletion of the *MYR1* locus in the Δ*myr1* line was confirmed by PCR (data not shown); Western blots using mouse antiserum raised to a recombinant MYR1 (representing amino acids 155 to 328 of the protein) (Fig. 2B; also, see Materials and Methods) further confirmed both the deletion and successful complementation (Fig. 3A).

HFFs were infected with the deleted and complemented parasites, and lysates of infected cells were prepared at 20 hpi. Wild-type and mock-infected cells served as positive and negative controls for c-Myc induction, respectively. The results (Fig. 3A) showed a much-reduced level of host c-Myc in cells infected with the Δ*myr1* parasites compared to cells infected with wild-type or complemented parasites, indicating that MYR1 is indeed necessary for c-Myc induction.

MYR1 is cleaved in a process dependent on *Toxoplasma*'s ASP5 protease. Although the MYR1 protein is predicted to be about 80 kDa after removal of the signal peptide, Western blots of purified wild-type RH (RH-WT) and RHΔ*myr1*::*MYR1* complemented parasites revealed two bands using the anti-MYR1 antibody that migrate as if they were ~105 kDa and ~80 k Da, respectively (Fig. 3B). Western blots of the C-terminally HA-tagged RHΔ*myr1*::*MYR1* line using anti-HA antibodies also yielded a band migrating at ~105 kDa, but instead of the ~80-kDa band, there was a band that migrated at ~32 kDa (Fig. 3C). Given that the recombinant protein used to generate the anti-MYR1 antibodies corresponded to the N-terminal portion (Fig. 2B), and the ~32-kDa band was detected only using the anti-HA antibodies and not with the anti-MYR1 antibodies, these results indicate that MYR1 is initially synthesized as a precursor that migrates as if it is ~105 kDa and that this protein is then proteolytically cleaved to yield fragments corresponding to about the N-terminal three-fourths and C-terminal one-fourth of the protein. The slow migration of the full-length MYR1 and the N-terminal three-fourths could be a result of posttranslational modifications and/or MYR1's acidic pI (~5.0).

Near the predicted cleavage site based on size is the amino acid sequence RRLSE (Fig. 2B). This is reminiscent of the *Plasmodium* export element, or PEXEL motif (28, 29), that is processed by plasmepsin V, an aspartyl protease in *Plasmodium* parasites (30–32). As recently shown by Coffey et al., aspartyl protease 5 (ASP5), a *Toxoplasma* orthologue of the *Plasmodium* plasmepsin, is necessary for MYR1 cleavage and mutation of the RRLSE sequence to ARLSE abrogates cleavage, strongly suggesting that MYR1 is cleaved by ASP5 within this pentapeptide, likely between the L and

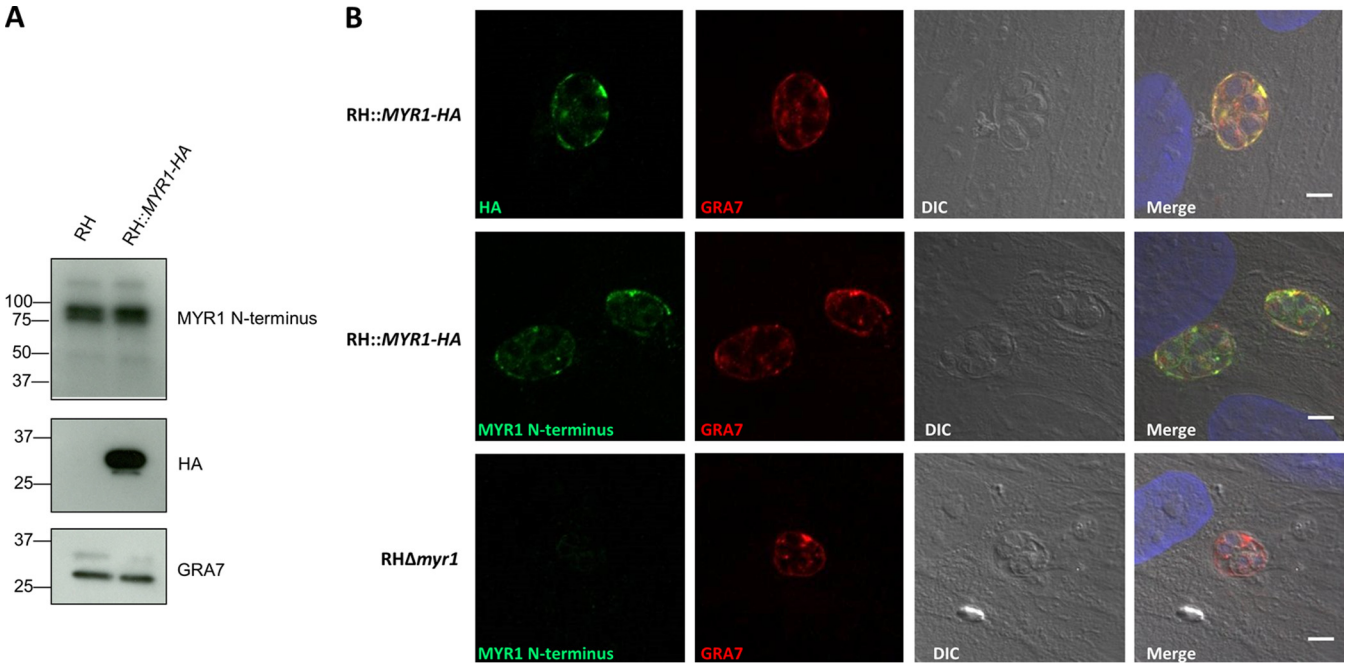

FIG 4 MYR1 N-terminal and C-terminal domains localize to the parasitophorous vacuole membrane and PV space. (A) C-terminal HA-tagging of the endogenous MYR1 locus does not affect its expression levels. Extracellular tachyzoites of the RH and C-terminally tagged RH:*MYR1-HA* strains were lysed in radioimmunoprecipitation assay (RIPA) buffer and analyzed by Western blotting using anti-MYR1(155–328) and anti-HA antibodies. GRA7 antibodies were used to assess equal loading. (B) The N-terminal and C-terminal domains of MYR1 localize to the PV and PVM. HFFs were infected with the RH:*MYR1-HA* strain and fixed with methanol at 12 hpi. The fixed monolayers were stained with DAPI and antibodies to HA or MYR1 N-terminus (green) and GRA7 (red).

S, based on the specificity of ASP5 (33). The role of this cleavage is not known, but it could be related to the trafficking and/or biochemical function of MYR1.

MYR1 is secreted into the PV and associates with the PVM. The complemented strain used in the studies described above used an ectopically expressed version of *MYR1*, driven off the *GRA1* promoter. GRA1 is a very abundantly expressed dense granule protein, and this strain served the purpose of showing that complementation of the Δ*myr1* mutant with ectopic *MYR1* rescues the c-Myc regulation phenotype. For determining the true localization of MYR1, however, we needed to be sure the protein was expressed at normal levels and at the correct time in the parasite's cell cycle. We therefore also created a strain where the native *MYR1* locus was engineered to encode a C-terminal HA tag (RH:*MYR1-HA*). Control experiments confirmed that the expression of this tagged MYR1 were comparable to the levels seen in wild-type parasites (Fig. 4A).

HFFs were infected with RH:*MYR1-HA*, fixed with methanol at 12 hpi, and examined by confocal microscopy using antibodies to the HA tag (to detect the C-terminal domain) or antibodies to the N-terminal rMYR1(155–328). Rabbit antibodies to GRA7 were used as a counterstain and a marker for a secreted protein. The results showed that, like GRA7, both the C- and N-terminal domains of MYR1 are abundantly present within the PV with rare puncta within the parasites themselves (Fig. 4B). Staining for both domains was also seen at the PVM, especially in cells that had vacuoles containing only one or two parasites. Colocalization with anti-GRA7 signal was seen in all three areas although the data did not allow us to reach a firm conclusion on whether MYR1 and GRA7 originate in the same structures (dense granules) within the parasite. This ambiguous, "dense-granule-like" staining is similar to what has been reported for GRA24 (8). Overall, however, these data clearly show that, like GRA7, MYR1 is a secreted protein and that both domains are present in the PV space, with a considerable amount at the PVM itself.

Consistent with these localization results, a recent phosphoproteomics study of tachyzoite-infected fibroblasts by Treeck et al. (24) indicated that MYR1 is specifically phosphorylated outside the parasite (i.e., within the PV and/or the infected host cytosol) (34). The positions of the four phosphorylated serines identified in that study are depicted in Fig. 2B.

MYR1 is necessary for *Toxoplasma*'s impact on host cell cycle. c-Myc is a potent transcription factor whose up-regulation likely affects the host cell in profound ways. One such impact might be on progression through the cell cycle, given c-Myc's demonstrated role in this key pathway (10, 11, 35–38). To examine this, we used propidium iodide to stain host cells that were first infected with either wild-type RH tachyzoites or RHΔ*myr1*. The results (Fig. 5) showed that relative to uninfected cells, RH infection results in a profound dysregulation of the host cell cycle, with many cells showing four times the normal complement of DNA, i.e., 8n. The ploidy profile of host cells infected with the Δ*myr1* mutants, on the other hand, was indistinguishable from that of uninfected cells. This indicates that MYR1 is needed for *Toxoplasma*'s ability to disrupt the host cell cycle, possibly through its role in the up-regulation of c-Myc. Alternatively, the role of MYR1 in this effect on host cell cycle could be through an indirect effect involving other parasite effectors or host proteins other than c-Myc.

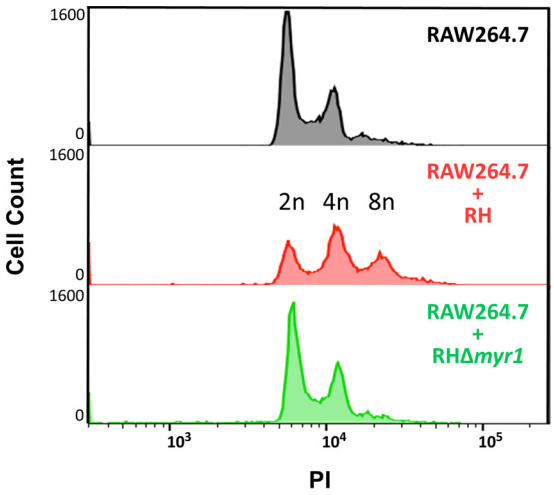

FIG 5 The cell cycle is dysregulated in cells infected by wild-type parasites but not in cells infected with Δ*myr1* mutants. Propidium iodide assessment of cell DNA content was performed in RAW264.7 cells at 19 hpi with RH and RHΔ*myr1* parasites expressing mCherry. Cells were fixed with methanol, stained with propidium iodide, and then assessed on an LSRII flow cytometer. The three peaks represent cells in G_0/G_1 (2n), cells in G_2/M (4n), and aneuploid cells (~8n).

MYR1 is dispensable for a subset of host interactions mediated by dense granule proteins. To better understand the function of MYR1 and to test the possibility that it is a part of the machinery that delivers or otherwise potentiates effectors rather than being an effector itself, we sought to determine whether the Δ*myr1* mutant was deficient in other host interactions, especially those mediated by known dense granule effectors. The first such process we tested was the phenomenon of host mitochondrial association (HMA) which we have previously reported to be mediated by a secreted dense granule protein known as MAF1 (mitochondrial association factor 1) (39). MAF1 is expressed by type I strains at the PV membrane (PVM), where it binds to host mitochondria. If MYR1 is involved in the trafficking or maturation of all dense granule proteins, then the Δ*myr1* mutants should be deficient in HMA. HFFs were therefore infected with wild-type RH, RHΔ*myr1*, and RHΔ*myr1*::*MYR*. As a control for the identity of the parasite lines, we first tested and confirmed that they had the expected phenotypes for c-Myc induction (Fig. 6A). Parallel infections were then fixed and assessed for mitochondrial recruitment by staining with anti-TOM20. The results (Fig. 6B) showed that the RHΔ*maf1* parasites exhibited the expected lack of HMA, whereas cells infected with the RHΔ*myr1* mutants showed strong HMA, indistinguishable from that of cells infected with wild-type parasites. These results were confirmed by electron microscopy (data not shown). Hence, MYR1 is not necessary for efficient HMA.

The next phenotype we tested was the ability to induce NF-κB nuclear localization. This is a trait of type II strains, not the more commonly studied type I strains such as RH, and is mediated by GRA15, which localizes to the PV after invasion (6). To determine whether MYR1 plays a role in GRA15's ability to induce NF-κB, we engineered a type II strain (ME49) that lacks MYR1 and then assessed this strain for its ability to cause up-regulation of NF-κB. The results (Fig. 6C) showed that the absence of MYR1 has no effect on the ability to induce NF-κB, further arguing that MYR1 is not part of the general machinery for dense granule protein synthesis, secretion, and subsequent translocation to the PVM.

MYR1 is necessary for the action of two dense granule proteins that cross the PVM and accumulate in the host nucleus. Some interactions of *Toxoplasma* tachyzoites are mediated by effectors that are translocated across the PVM and then act within the host nucleus, one example being GRA24, which mediates the sustained activation of p38 MAP kinase (8). To test if MYR1 impacts such an effector, we asked whether MYR1 is necessary for tachyzoites to activate host p38 MAPK relative to infection. The results (Fig. 7A and D) showed that the RHΔ*myr1* mutant is indeed unable to cause substantial activation of p38, indicating a role for MYR1 in this process. Although we cannot exclude the possibility that MYR1 is an accessory effector that works in partnership with GRA24, the fact that ectopic expression of GRA24 alone in uninfected cells can induce the changes in p38 (8) argues against the possibility of an accessory factor and suggests, instead, that MYR1 is part of the machinery necessary for maturation and/or translocation of GRA24 across the PVM.

GRA16 is another dense granule effector that traffics to the host cell nucleus, in this case intersecting with p53 and PP2A phosphatase pathways (7). To determine if MYR1 is necessary for the function of this effector, we assessed the ability of the RHΔ*myr1* mutant to induce PP2A-PR55B translocation from the cytosol to the nucleus in infected cells. The results (Fig. 7B and E) showed that the RHΔ*myr1* mutant is indeed defective in this respect, while the RHΔ*myr1*::*MYR1* complemented strain exhibited a rescued (wild-type) phenotype. These results are consistent with a general role in the maturation and/or trafficking of dense granule effectors that are transported across the PVM and reach the host cytosol.

The final host interaction assessed was the ability of *Toxoplasma* tachyzoites to specifically block the up-regulation and nuclear translocation of IRF1 in response to IFN-γ. This ability is a property of all three major strains (40), but the effector involved has not been identified. To test if MYR1 affects this pathway, we infected host cells with RH-WT or RHΔ*myr1* strains and then performed immunofluorescence assays using antibodies to IRF1. The results (Fig. 7C and F) showed that the RHΔ*myr1* mutants are completely defective in their ability to suppress the IRF1 response. To prove that this was related to the absence of MYR1, the RHΔ*myr1*::*MYR1* complemented strain was examined and found to rescue the defect. Hence, either MYR1 is the effector responsible for IRF1 up-regulation, or, like GRA16 and GRA24, the effector involved is dependent on MYR1 for its functionality.

MYR1 is necessary for trafficking of GRA24 to the host nucleus. To directly test if MYR1 plays a role in the trafficking of *Toxoplasma*'s exported effectors, we examined the location of GRA24 in the RHΔ*myr1* mutants by immunofluorescence analysis of infected cells. To do this, we introduced a plasmid expressing an epitope-tagged GRA24 into the RH-WT, RHΔ*myr1* and RHΔ*myr1*::*MYR1* strains and then stained the infected cells at 20 hpi. The results (Fig. 8) showed that the RHΔ*myr1* mutants are indeed defective in their ability to traffic GRA24 to the host nucleus, whereas RH-WT and the RHΔ*myr1*::*MYR1* complemented strains show efficient translocation. This indicates that MYR1 plays a crucial role in the physical translocation of GRA24 from the PV into the host cell.

MYR1 mutants exhibit no growth defect *in vitro* but have decreased virulence in mice. Given MYR1's involvement in sev-

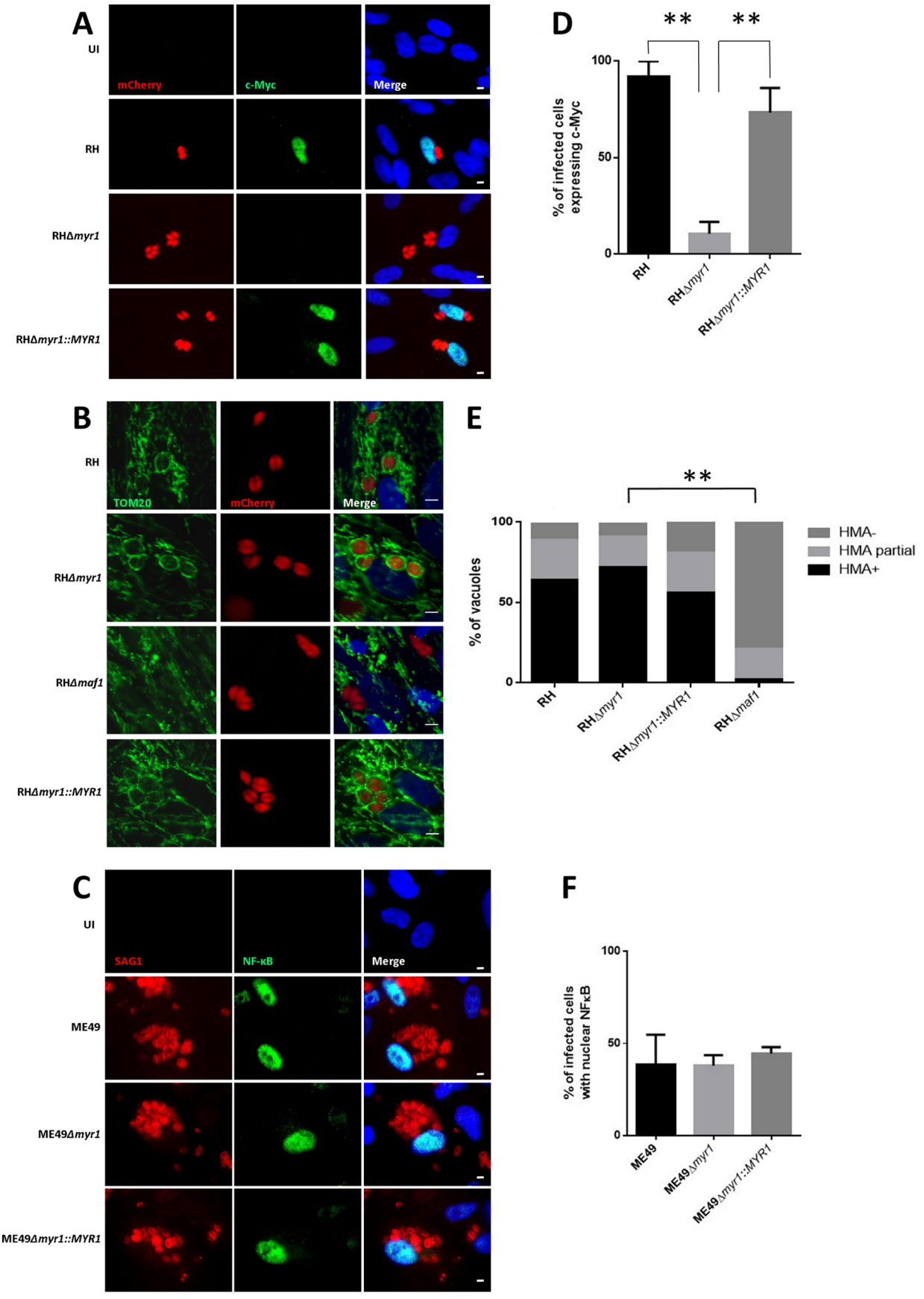
A
UI
mCherry
c-Myc
Merge
RH
RHΔmyr1
RHΔmyr1::MYR1
B
RH
TOM20
mCherry
Merge
RHΔmyr1
RHΔmaf1
RHΔmyr1::MYR1
C
UI
SAG1
NF-κB
Merge
ME49
ME49Δmyr1
ME49Δmyr1::MYR1
D
**
**
% of infected cells expressing c-Myc
100
50
0
RH
RHΔmyr1
RHΔmyr1::MYR1
E
**
% of vacuoles
100
50
0
HMA-
HMA partial
HMA+
RH
RHΔmyr1
RHΔmyr1::MYR1
RHΔmaf1
F
% of infected cells with nuclear NFκB
100
50
0
ME49
ME49Δmyr1
ME49Δmyr1::MYR1

eral key pathways involving interactions with the host, we assessed its growth phenotype *in vitro* and virulence *in vivo*. The ability of the Δ*myr1* parasites to grow in HFFs *in vitro* was first measured. The results (Fig. 9A and C) showed that growth of both the RHΔ*myr1* and ME49Δ*myr1* parasites *in vitro* was indistinguishable from that of wild-type RH and ME49, respectively, consistent with the fact that the pathways shown here to be dependent on MYR1 are generally dispensable for growth in HFFs.

To determine if the mutants had a defect *in vivo*, C57BL/6 mice were infected intraperitoneally (i.p.) with ME49, ME49Δ*myr1*, or the complemented strain ME49Δ*myr1*::*MYR1*, and survival and weight loss were assessed. The results (Fig. 9B) showed that all mice infected with wild-type ME49 parasites succumbed by 9 days postinfection (dpi), whereas all of the mice infected with ME49Δ*myr1* mutant parasites survived. Similar results were obtained with the RH lines, except that the effect of lacking MYR1 was less dramatic with a reproducible delay only in the mean time to death: infection with the wild type and the complemented RH lines resulted in death by 9 to 10 dpi, versus days 10 to 13 for the RHΔ*myr1* line (Fig. 9D). All infected mice (including the RHΔ*myr1*-infected mice) underwent rapid weight loss (an expected symptom in mice infected with *Toxoplasma*) after about day 5 (data not shown). Thus, MYR1 is necessary for full virulence and is especially important in mouse infections with type II strains.

DISCUSSION

Using reporter cells from transgenic mice with a c-Myc–GFP fusion, we were able to isolate *Toxoplasma* mutants deficient in the induction of host c-Myc. Three such mutants were characterized, and all were found to be deficient in a single secreted protein, dubbed MYR1. Detailed phenotyping of Δ*myr1* mutants showed a profound defect in the induction of not only host c-Myc but also several other phenotypes involving interaction with the host, including the GRA16-mediated translocation of PP2A, the GRA24-mediated phosphorylation of p38 MAPK, and the induction of IRF1 in the presence of IFN-γ, mediated by an as-yet-unidentified effector. Interestingly, however, the Δ*myr1* mutants were not defective in host mitochondrial association or NF-κB activation, processes mediated by the dense granule proteins MAF1 and GRA15, respectively. These findings argue that MYR1's role is for only a subset of the effectors that originate in dense granules. MAF1 is known to operate at the PVM, and GRA15's final location is not known (it has never been observed outside the PV/PVM), whereas GRA16 and GRA24 clearly traffic to the host nucleus (7, 8). It appears, therefore, that MYR1 functions only in the trafficking of dense granule proteins that physically translocate, in their entirety and as soluble entities, across the PVM.

Our data do not address when or where MYR1 is cleaved into its two domains, and the fact that both give an indistinguishable signal by IFA leaves open the possibility that the cleavage occurs after release from the parasites. The fact that ASP5, the enzyme apparently responsible for the cleavage (33), is found within the Golgi apparatus (33, 41, 42), however, strongly suggests that cleavage occurs prior to release and that the two domains either remain associated or independently target the same ultimate location in the PV/PVM. Both the N- and C-terminal domains are abundant within the PV. The presence of two predicted TM domains in the C-terminal domain strongly suggests that MYR1 is integral to a membrane, likely some combination of the membranous nanotube system of the intravacuolar network and the PVM, both of which appear normal by electron microscopy in the RHΔ*myr1* mutants (S. Rastogi and M. Panas, unpublished data). Such an association is consistent with the role of MYR1 in translocating proteins into the host cytosol.

The splicing of the *MYR1* transcript appears to differ somewhat between strains based on RNA-Seq data from many labs available on ToxoDB: in lab strains that have been passaged *in vitro* for many years, such as the common RH, GT1, and ME49 strains, the intron is removed in about 50 to 70% of the 254,470 mRNA species. In "wild" isolates that have not been passaged routinely in the lab, such as the ~20 field isolates analyzed by Minot et al. (43) and the type II Czech isolate used for studies of sexual differentiation in cats (44), this first intron is rarely if ever spliced out. As noted above, splicing out this intron results in a protein that lacks the first 78 amino acids compared to the version encoded by the mRNA with this intron intact, and the resulting N-terminally truncated version of MYR1 would lack a predicted signal peptide and thus presumably not be secreted. This suggests that there may be some cost to secreting a large amount of MYR1 and that repeated passage *in vitro* selects for decreased expression of secreted MYR1, perhaps because MYR1-mediated transport of effectors into the host cell is crucial only *in vivo*, where manipulation of the host's immune response is required.

The precise role played by MYR1 in mediating the effects of GRA16 and GRA24, including transit of GRA24 to the host nucleus, is not clear. Interestingly, BLAST analysis of just the C-terminal domain of MYR1 showed that outside *Toxoplasma*, *Hammondia*, and *Neospora*, the top two matches were a hypothetical protein of *Pseudomonas brasilianum* (PMG1108784; *E* value, 0.005) and TatC, a "Sec-independent periplasmic protein translocase" of *Halorhabdus utahensis* (*E* value, 0.64). TatC is part of a complex involving two other proteins, TatA and TatB, that translocates folded proteins containing a twin-arginine motif in their signal peptide across a membrane in a Sec-independent manner (45). This system is evolutionarily conserved, being present in archea, bacteria, chloroplasts, and plant mitochondria. Given that MYR1 appears to play a role in translocating proteins across a membrane (the PVM), and the putative homology was in the region that includes the two predicted transmembrane domains of MYR1, it is tempting to speculate that MYR1 is indeed a homo-

FIG 6 MYR1 is not necessary for the ability of *Toxoplasma* tachyzoites to recruit host mitochondria or induce NF-κB. (A) Confirmation of c-Myc phenotype. HFFs grown in low-serum medium were infected with the indicated parasites expressing mCherry for 14 h before being fixed with formaldehyde and stained with DAPI and antibodies to c-Myc. UI, uninfected. Bar, 5 μm. (B) Effect of MYR1 on host mitochondrial association. The images are as described for panel A except that HFFs were infected with the indicated *Toxoplasma* strains for 13 h. Host cell mitochondria were detected using an anti-TOM20 antibody (green), and parasites were detected using the constitutively expressed mCherry marker in each strain (red). (C) Effect of MYR1 on nuclear NF-κB accumulation. The images are as described for panel A except that ME49, ME49Δ*myr1*, and ME49Δ*myr1*::*MYR1* parasites were used to infect HFFs for 30 h, at which time cells were fixed and stained with anti-SAG1 antibody (red) and anti-NFκB antibody (green). (D, E, and F) c-Myc induction, HMA, and nuclear NF-κB accumulation were quantified. Data are means and standard errors of the means (SEM) from three independent assessments. **, $P < 0.01$.

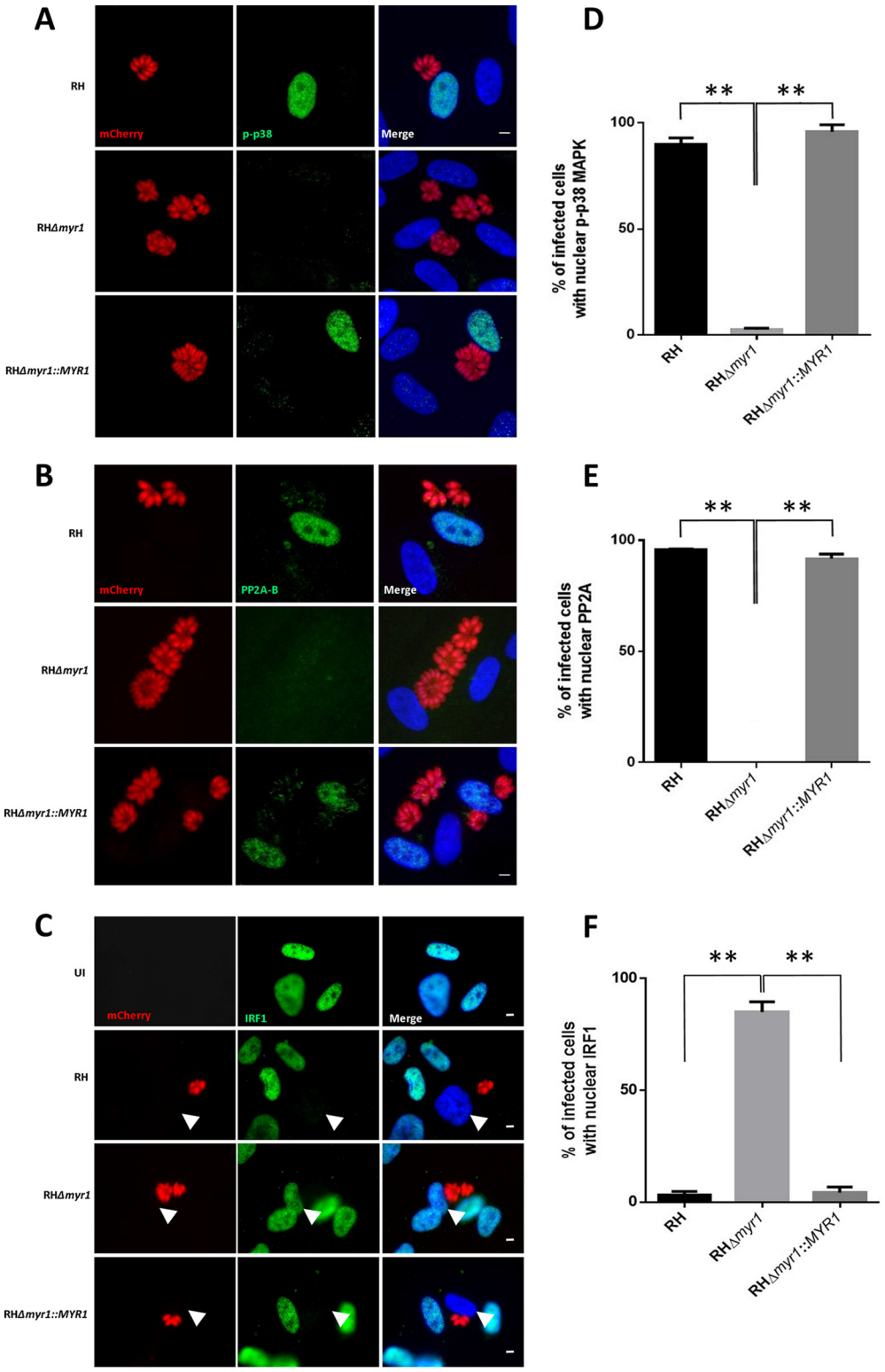

FIG 7 MYR1 is necessary for the function of several effectors, including GRA16 and GRA24. (A) Effect of MYR1 on GRA24-mediated p38 MAPK activation. An immunofluorescence assay was performed on confluent HFFs that were uninfected or infected with the indicated strains. At 20 hpi, cells were fixed and stained using anti-phospho-p38 MAPK antibody. Bar, 5 μm. (B) Effect of MYR1 on GRA16-mediated PP2A nuclear translocation. The images are as described for panel A except that cells were stained using antibody to the PP2A-B subunit. (C) Role for MYR1 in the block of IFN-γ-induced IRF1 activation. The images are as described for panel A except that HFFs were infected for 14 h with the indicated parasites expressing mCherry, stimulated with 200 units/ml of IFN-γ for 6 h, and fixed with formaldehyde. Cells were stained using anti-IRF1 antibody. White arrowheads highlight the host nuclei in infected cells. UI, uninfected. (D, E, and F) p38 phosphorylation and nuclear accumulation, PP2A nuclear translocation, and IRF1 nuclear accumulation were quantified. Data are means and SEM from three independent assessments. **, $P < 0.01$.

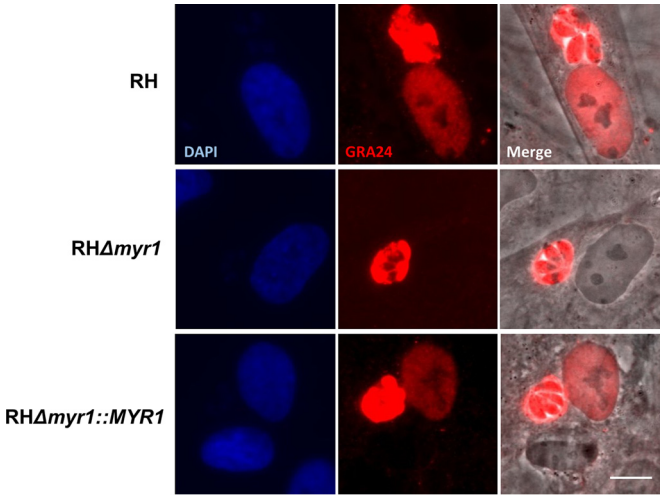

FIG 8 MYR1 plays a role in translocation of GRA24 to the host nucleus. HFFs were infected with RH-WT, RHΔ*myr1*, or RHΔ*myr1*::*MYR1* parasites expressing a Myc-tagged GRA24, and at 20 hpi, the cultures were fixed and stained with antibodies to the Myc tag. Bar, 5 μm.

logue of TatC, even though the *E* value was weak. BLAST analysis of the *Toxoplasma* genome with the TatA and TatB proteins did not reveal any apparent homologues (data not shown), but given the very weak extent of similarity between MYR1 and TatC, orthologues may not be readily detected by this method. Future studies aimed at isolation of MYR1-associated proteins will help address this and the question of whether the N- and C-terminal domains of MYR1 associate in infected cells.

Our data do not address whether one or both portions of MYR1 are necessary for the c-Myc up-regulation and the other MYR1-dependent phenotypes described here. Given the tantalizing similarity of the C-terminal domain to TatC, we attempted to ectopically express this domain, including the ASP5-dependent cleavage site, fused to the MYR1 signal peptide, but the resulting protein was not stably expressed. It may be that proper folding, secretion, and/or localization within the PV/PVM of both domains is dependent on their being synthesized as a single protein to start.

Our results showing attenuated virulence of the Δ*myr1* mutants indicate a role for MYR1 in the pathogenesis of *Toxoplasma* in mice, especially for type II strains like ME49. While not directly demonstrated, such a role for MYR1 seems likely to be through its impact on several key pathways that *Toxoplasma* tachyzoites disrupt in the infected cell: c-Myc, p53, p38 MAPK, and IRF1. All these data are consistent with the fact that MYR1 is dispensable for growth *in vitro*.

No obvious orthologue of *MYR1* is detectable in the related parasite *Plasmodium falciparum*, which is also known to translocate proteins across the PVM, in this case into the erythrocyte cytosol (13–15). This suggests that either the machinery has di-

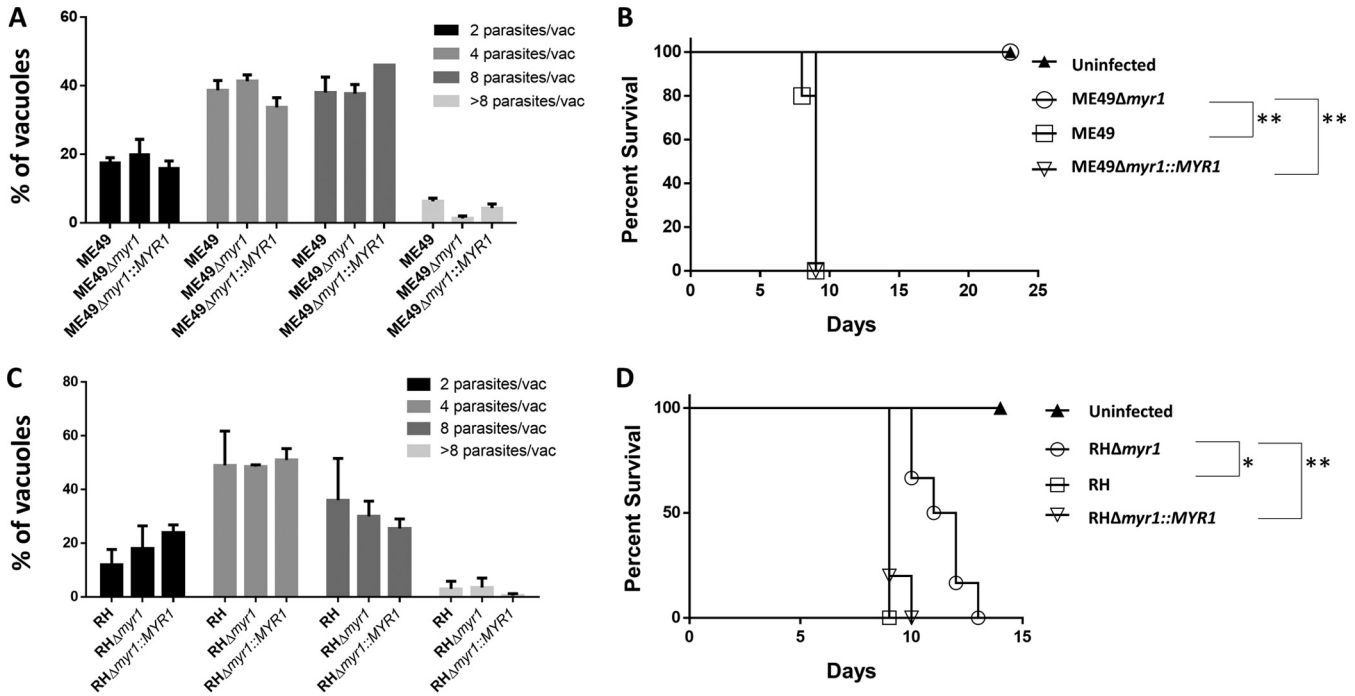

FIG 9 MYR1 mutants exhibit wild-type growth *in vitro* but decreased virulence in mice. (A) Growth comparison of ME49 strains *in vitro*. HFF were infected with the indicated strains of parasites for 22 h, and the number of parasites in each vacuole was then assessed. The percentage of vacuoles demonstrating 2, 4, 8, or >8 parasites per vacuole is displayed. Data are averages for two independent replicates. (B) Kaplan-Meier survival curve for mice infected with ME49 parasites with or without MYR1. Five mice in each group were injected intraperitoneally with PBS or with 100 tachyzoites of *Toxoplasma* ME49, ME49Δ*myr1*, or ME49Δ*myr1*::*MYR1*. The results are representative of two experiments with similar outcomes. (C) As for panel A, growth of RH strains was assessed in HFFs at 16 h. The percentage of vacuoles demonstrating 2, 4, 8, or >8 parasites per vacuole is displayed. Data are averages for two independent replicates. (D) As for panel B, survival was assessed in mice injected intraperitoneally with PBS or with 100 tachyzoites of *Toxoplasma* RH (5 mice per group), RHΔ*myr1* (6 mice per group), or RHΔ*myr1*::*MYR1* (5 mice per group). The results are representative of two experiments with similar outcomes. *, $P < 0.05$; **, $P < 0.01$.

verged in sequence to the extent that it is no longer identifiable by BLAST or different machinery suffices for this purpose. Indeed, *Plasmodium* spp. are known to use a PTEX complex for translocating proteins across the PVM (13–15), and so perhaps that machinery functions without the need for a MYR1-like protein. *Toxoplasma* encodes a clear orthologue of at least one of the key components of the PTEX, EXP2 (GRA17 in *Toxoplasma*), but this protein has recently been shown to function in translocation of only small molecules (under 3,000 Da), not proteins, across the PVM (16), and so evidence for a PTEX-like machine for proteins in *Toxoplasma*-infected cells does not yet exist. It seems, instead, that the different selective pressures operating in the host cells occupied by *Toxoplasma* and *Plasmodium* (most nucleated cells and erythrocytes, respectively) may have resulted in the evolution of distinct translocation systems for these two important parasites.

All three mutants produced by our screen and selected for further analysis were defective in MYR1. While this indicates that MYR1 is a major player in the phenotype that was the basis of our screen (up-regulation of c-Myc upon *Toxoplasma* infection), it does not exclude the possibility that mutations in other key genes will be among the other mutants obtained but not yet characterized. Indeed, the recent results of Coffey et al. showing that the Δ*asp5* mutant is defective in c-Myc up-regulation (33) predicts that, were it not for their growth defect *in vitro*, *ASP5* mutants should be present in our mutant set. Given the pleiotropic phenotype of the Δ*myr1* mutants, MYR1 seems unlikely to be the actual effector driving c-Myc up-regulation, and so these other mutants may lead us to that effector. It is also possible that c-Myc up-regulation is a somewhat redundant process involving more than one effector, in which case mutations in machinery like MYR1 might give rise to a stronger phenotype than those in a single effector, and this would explain why all 3 mutants first examined had mutations in this gene. Extensive analysis of the other mutants obtained will help answer this question.

Overall, the results presented here show that a novel exported protein of *Toxoplasma gondii* is necessary for the function of several secreted effectors and that the absence of this protein results in a substantial attenuation of virulence in mice. The mechanism by which this protein functions is not yet known, but the data strongly suggest that it is involved in the transport of effectors across the PVM, where they can then access other compartments in the host cell.

MATERIALS AND METHODS

Parasite strains, culture, and infections. The following strains were used in this study: *Toxoplasma gondii* RH CRE-toxofilin mCherry (46), *Toxoplasma gondii* ME49-*luc*Δ*hxgprt* (47), and *Neospora caninum* NC-1 mCherry (9). *Toxoplasma* and *Neospora* tachyzoites were propagated in human foreskin fibroblasts (HFFs) cultured in complete Dulbecco's modified Eagle medium (cDMEM) supplemented with 10% heat-inactivated fetal bovine serum (FBS), 2 mM L-glutamine, 100 U ml^{-1} penicillin, and 100 μg ml^{-1} streptomycin. Prior to infection, parasites were scraped and lysed using a 27-gauge needle, counted using a hemocytometer, and added to HFFs. Mock infection was done by syringe-lysing uninfected HFFs, processing them in the same manner as the infected cells, and then adding the same volume of the resulting material as used for infections.

ENU mutagenesis. *Toxoplasma* RH CRE-toxofilin mCherry parasites were grown in HFFs to full vacuoles and treated with cDMEM containing 1 mM *N*-ethyl-*N*-nitrosourea (ENU). After a 2-h incubation at 37°C, mutagenized cells were washed three times for 10 s at room temperature by rinsing the monolayer with 10 ml cold 1× phosphate-buffered saline (PBS), scraped, syringe-lysed into 3 ml PBS, counted, and added to a new flask with HFFs. Mutagenized parasites were expanded for 24 h in HFFs prior to screening for c-Myc mutants. The percent killing that resulted from ENU mutagenesis was assessed by counting plaques resulting from mutagenized and dimethyl sulfoxide (DMSO)-treated parasites. Briefly, 100 parasites were added to a flask containing an HFF monolayer, and plaques were counted after 10 days of incubation at 37°C.

BMM isolation, culture, and infection. Mouse bone marrow macrophages (BMMs) were derived from the femurs and tibias of mice via culture for 8 days in cDMEM plus 20% (final concentration) macrophage colony-stimulating factor (M-CSF)-containing medium. Expanded BMMs were infected with *Toxoplasma* or *Neospora* parasites at an MOI of 0.25 and incubated for 20 h at 37°C. Infected cells were washed and incubated in 1× PBS at 4°C for 10 min. BMMs were then harvested by scraping, centrifuged, resuspended in 250 μl PBS containing 0.5% FBS, and filtered using tubes with cell strainer caps (BD Biosciences). Flow cytometry analysis was performed as described below.

Flow cytometry. Infected cells were harvested by washing once with PBS and treating with trypsin for 5 min at 37°C. After one PBS wash, cells were resuspended in 0.5% FBS-PBS and filtered using tubes with cell strainer caps (BD Biosciences). Fluorescence was detected by the Falstaff BD Aria II sorter (Stanford FACS facility). Flow cytometry data were analyzed using FlowJo.

Whole-genome sequencing. Isolated mutant populations were singly cloned by limiting dilution followed by expansion in HFFs. Genomic DNA from three mutant strains and a wild-type strain was isolated using genomic DNA Clean & Concentrator (Zymo Research).

For the DNA library preparations, 1 μg of gDNA was first sheared down to 200 to 300 bp using the Covaris S2 per the manufacturer's recommendations. Paired-end sequencing libraries were prepared using Illumina's TruSeq PCR free sample preparation kit. The target insert size of 200 to 250 bp was size selected using SPRI Ampure XP purification. Following DNA library construction, library size distribution was checked using the Agilent Bioanalyzer high-sensitivity assay. Library quantification was done via qPCR (Stratagene MX3005P). DNA libraries were sequenced using the Illumina HiSeq 2000 in one lane on a flow cell with sequencing paired-end read length at 2 × 50 bp. Reads were demultiplexed using CASAVA (version 1.8.2).

DNA sequencing data processing and SNV analysis. The DNA sequencing reads in Fastq format were first checked for quality using FastQC (http://www.bioinformatics.babraham.ac.uk/projects/fastqc). Sequencing adapter sequences present in the reads were trimmed using SeqPrep (https://github.com/jstjohn/SeqPrep). Sequencing reads were then mapped using Bowtie2 (48) with default parameters against the reference genome of *Toxoplasma gondii* GT1 strain downloaded from ToxoDB (release 10.0) (49). Single nucleotide variants (SNVs) that were present in mutant strains and not in the wild type were identified using RADIA (https://github.com/aradenbaugh/radia/) (50). RADIA used the SAMtools (51) (mpileup command [version 0.1.18]) to examine the base calls at each locus of the genome in parallel for the wild type and the mutant sample. The BAM files generated by Bowtie2 were used as input, and output variants were in variant call format (VCF) (https://github.com/samtools/hts-specs). For each base, the following cutoffs were used: a minimum Phred base alignment score of 10 and a minimum Phred mapping quality score of 10. Additional SNV filtering steps were a requirement for an overall read depth of 10 for both the wild type and the mutant strain and a minimum read depth that supported the alternative allele of 4 and 80% of the total read depth.

Western blotting. Cell lysates were prepared at 20 h postinfection (hpi), and the total protein concentration of lysates was determined by a Bradford protein assay (Bio-Rad). Samples containing 20 μg of protein were boiled for 5 min, separated by SDS-PAGE, and transferred to polyvinylidene difluoride (PVDF) membranes. c-Myc was detected by incubation of membrane with rabbit anti-N-terminus c-Myc antibody (Y69;

Abcam) and followed by incubation with horseradish-peroxidase conjugated goat anti-rabbit IgG. The levels of horseradish peroxidase (HRP) were detected using an enhanced chemiluminescence (ECL) kit (Pierce). The expression of MYR1 in parasite strains was detected using mouse anti-MYR1 primary antibodies or anti-hemagglutinin (anti-HA) antibodies (in complemented parasites) and secondary goat anti-mouse IgG. Host GAPDH levels served as a loading control: membranes were stripped with stripping buffer (Thermo Scientific) and stained with mouse anti-GAPDH primary antibody and secondary HRP-conjugated goat anti-mouse IgG antibody. The levels of HRP were measured as stated above. SAG1 levels were used to control for the levels of parasites within the infected cells. Again, membranes were stripped with stripping buffer and stained with rabbit anti-SAG1 followed by staining with secondary HRP-conjugated goat anti-rabbit IgG antibody and detecting the levels of HRP as described above.

Generation of RHΔ*myr1* and ME49Δ*myr1* parasites. To generate RHΔ*myr1* parasites, the parental RHΔ*hxgprt* strain, deficient in the hypoxanthine-xanthine-guanine phosphoribosyl transferase (HXGPRT) gene, was used (52). Previously described pTKO2 vector (53), which carries the *HXGPRT* gene flanked by *loxP* sites, was modified by flanking the *HXGPRT* gene with sequences that correspond to 5′ and 3′ genomic regions adjacent to the *MYR1* open reading frame (ORF) (*TGGT1_254470*). First, the right flank (3′ region) was cloned into the pTKO2 vector. This region of about ~1.2 kb was amplified from RH genomic DNA by PCR using the primers 5′-GCGCAAGCTTCGAGAGACAAATTATCCAGCA TTGATTC-3′ (forward) and 5′-GCGCGCTAGCCCTTGTCTCTGTGT GCAGCGC-3′ (reverse). The resulting DNA fragment was then inserted into the 3′ multiple cloning site (MCS) flanking the *HXGPRT* gene in pTKO2 vector using HindIII and NheI restriction sites. Next, the 5′ flanking region of ~1.5 kb was generated using the following primers: 5′-GCG CGGTACCCGCCCTGCAGGTTGAAGAACGT-3′ (forward) and 5′-GC GCCTCGAGTTCCCTCTCCTGATAACAGCTAGC-3′ (reverse). This region was cloned into the 5′ MCS of the pTKO2 vector using KpnI and XhoI restriction enzymes. Twenty-five micrograms of the resulting non-linearized pTKO2_MYR1_KO plasmid was transfected into RHΔ*hxgprt* parasites via electroporation. Transfected parasites were cultured in HFFs grown in 24-well plates, and after 24 h, their medium was replaced with selective medium containing 50 μg/ml mycophenolic acid and 50 μg/ml xanthine to select for parasites expressing HXGPRT. After two passages in selective medium, parasites were single-cell cloned by limiting dilution. The resulting parasite strains were tested for HXGPRT integration at the 5′ and 3′ ends, and the absence of *MYR1* was confirmed by PCR using primers homologous to the *MYR1* open reading frame (data not shown). Ultimately, the loss of MYR1 expression in parasites was confirmed by Western blotting using the mouse anti-MYR1 antibody (Fig. 3). To generate ME49Δ*myr1*, the above-described transfection was repeated using ME49-*luc*Δ*hxgprt* (the HXGPRT-deficient type II ME49 strain that expresses firefly luciferase). The same pTKO2_MYR1_KO vector was used to delete MYR1 in ME49-*luc*Δ*hxgprt* and RHΔ*hxgprt* parasites.

Ectopic complementation of RHΔ*myr1* and ME49Δ*myr1* parasites. To ectopically complement RHΔ*myr1* parasites, the *HXGPRT* selection marker flanked by *loxP* sites was first removed from the knockout parasites via CRE-mediated DNA recombination as previously described (53). Briefly, *myr1*-deficient parasites were transiently transfected with a vector carrying CRE recombinase, and Δ*hxgprt* parasites were selected using cDMEM supplemented with 350 μg/ml 6-thioxanthine. Parasites were then single-cloned by limiting dilution and the loss of HXGPRT was confirmed by their inability to grow in media supplemented with mycophenolic acid/xanthine. The resulting RHΔ*myr1*Δ*hxgprt* strain was then used to generate the complemented RHΔ*myr1*::*MYR1* parasites by transfecting with a vector carrying the coding region of RH *MYR1*. This vector was generated by modifying the pGRA1_HA_HXGPRT vector (54): the open reading frame (ORF) of MYR1 lacking the stop codon was amplified from RH genomic DNA using the following primers: 5′-GCGCATGCATATG CGATGCCTAGTGGCTCTTC-3′ (forward) and 5′-GCGCCCATGGCG AATTATGTGACTGACGGAAATGACG-3′ (reverse). The resulting ~4.4-kb fragment was digested with NsiI and NcoI and cloned into the pGRA1_HA_HXGPRT vector. RHΔ*myr1*Δ*hxgprt* parasites were transfected with 15 μg of the newly synthesized pGRA1_MYR1_HA_HXGPRT vector, and HXGPRT$^+$ parasites were selected using MPA/XAN selective medium as described above. MYR1 expression in cloned parasites was confirmed by Western blotting using anti-MYR1 and antihemagglutinin (anti-HA) antibodies.

To generate ME49Δ*myr1*::MYR1 complemented parasites, the above-described steps were repeated using the ME49Δ*myr1* strain, except that the coding region of MYR1 was amplified from the ME49 genomic DNA using the primers described above.

C-terminal HA-tagging at the endogenous *MYR1* locus. To construct the vector pTKO2_MYR1_HA for C-terminal endogenous HA-tagging of MYR1, approximately 3,000 bp of the MYR1 3′ coding sequence and hemagglutinin (HA) tag were amplified from the pGRA1_MYR1_HA_HXGPRT complementation plasmid using the primers 5′-GCGCGCGGCCGCCTGTGGAGCGTAGCCAATGATTTT C-3′ and 5′-GCGCGATATCCTACGCGTAGTCCGGGACGT-3′. The resulting insert was cloned into NotI and EcoRV sites of the pTKO2 mCherry vector. The plasmid was linearized at the SmaI site in the insert, and 25 μg of the linearized plasmid was transfected by electroporation into the RHΔ*ku80*Δ*hpt* strain. Parasites were allowed to infect HFFs in T25 flasks for 24 h, after which the medium was changed to complete DMEM supplemented with 50 μg/ml MPA and 50 μg/ml XAN for HXGPRT selection. Parasites were passaged twice before being singly cloned into 96-well plates by limiting dilution. Screening for correct integration into the endogenous locus was performed by PCR using multiple primers, including 5′-GATTCCCCCACCTTCTCAGACCAT-3′ and 5′-GCGCgat atcCTAcgcgtagtccgggacgt-3′, as well as by Western blotting.

Generation of polyclonal anti-MYR1 antibodies. N-terminal glutathione *S*-transferase (GST)-fused proteins were expressed using the pGEX-6P1 plasmid (Agilent Technologies). The N-terminal exon region of MYR1 was amplified using the primers 5′-AGAATTCCTAGACCGAC AAGACCAG-3′ and 5′-AGCGGCCGCTTCAGGGCACACGAGATCG C-3′ (corresponding to amino acids 155 to 328, inclusive). The resulting recombinant protein was purified from *Escherichia coli* (Rosetta strain; Novagen/EMD Millipore) and injected intraperitoneally into female BALB/c (Charles River) mice with a Sigma Adjuvant System (Sigma) according to the manufacturer's instructions. Blood of naive mice was drawn prior to injection, and mice with sera that exhibited the lowest baseline reactivity against monolayers of *Toxoplasma*-infected cells were selected for antibody generation. Mice were injected with the initial dose of 100 μg protein/mouse followed by boosters of 50 μg protein/mouse on days 21, 40, 65, and 89 after the initial injection. Serum from these mice was isolated on days 33, 51, 75, and 113 after the initial injection. All animal experiments were conducted with the approval and oversight of the Institutional Animal Care and Use Committee at Stanford University.

Immunofluorescence microscopy. Infected cells grown on glass coverslips were fixed using 2.5% formaldehyde in PBS for 20 min or using methanol, as indicated in the text. Samples were washed one to three times with PBS and blocked using 3% bovine serum albumin (BSA) in PBS for 1 h at room temperature. Cells were permeabilized with 0.2% Triton X-100–3% BSA–PBS for 10 min at room temperature. MYR1 protein was detected with mouse anti-MYR1 or rat anti-HA primary antibodies and secondary antibodies conjugated to 488-nm fluorochrome. c-Myc was labeled using rabbit anti-c-Myc antibodies and 488-nm-fluorochrome-conjugated goat anti-rabbit IgG. GRA7 protein was detected by mouse anti-GRA7 and 594-nm-fluorochrome-conjugated goat anti-rabbit IgG. NF-κB was detected with SC-109 (Santa Cruz Biotechnology). To assess host mitochondrial association, infected cells were fixed 12 to 14 hpi using 2.5% formaldehyde diluted in prewarmed medium and then permeabilized and blocked as described above. Mitochondria were detected with a

rabbit anti-TOM20 antibody (Santa Cruz Biotechnology) used at 1:100. Phospho-p38 MAP kinase and PP2A-B subunit were labeled using rabbit anti-phospho-p38 (Thr180/Tyr182) antibody (no. 9211; Cell Signaling Technologies) and rabbit PP2A B subunit antibody (no. 4953; Cell Signaling Technologies), respectively, followed by 488-nm-fluorochrome-conjugated goat anti-rabbit IgG. Vectashield with 4′,6-diamidino-2-phenylindole (DAPI) stain (Vector Laboratories) was used to mount the coverslips on slides. Fluorescence was detected using either wide-field fluorescence microscopy or by confocal microscopy using an LSM510 or LSM710 inverted confocal microscope (Zeiss). Images were analyzed using ImageJ or FIJI. All images shown for any given condition or staining in any given comparison or data set were obtained using identical parameters.

Cell cycle assessment. RAW264.7 murine macrophage-like cells were infected with parasites at an MOI of 3. At 19 h, cells were harvested and split into two populations, one to assess infection rate and one to assess cell cycle. Infection rates were approximately 97%. Cells intended for cell cycle analysis were fixed and permeabilized with methanol for 20 min and then stained with propidium iodide for 30 min before being assessed on an LSRII flow cytometer.

IRF1 staining. HFFs were infected at an MOI of 0.1 for 14 h before 200 units/ml of human IFN-γ was added. Six hours after the addition of IFN-γ, cells were fixed with formaldehyde and stained with the mouse monoclonal antibody clone 20/IRF1 (catalogue no. 612046; BD Biosciences, San Jose, CA, USA).

GRA24 localization. Tachyzoite-infected HFFs were scraped and lysed using a 27-gauge needle and spun down, and the parasites were then electroporated with 50 μg of the pHTU-GRA24-3XMyc plasmid expressing C-terminally Myc-tagged GRA24 off the tubulin promoter (33). The transfected and mock-transfected parasites were allowed to infect confluent HFFs for 20 h before the monolayers were fixed with 3% formaldehyde and stained using Myc-tag antibody (M4439; Sigma).

Mouse infections. Tachyzoites were grown in HFFs and isolated from infected cells by scraping of the cell monolayer and syringe lysis using a 27-gauge blunt needle. After one wash in PBS, parasites were counted and diluted in PBS. Female C57BL/6 mice were used for studies with ME49 parasites, and female CBA/J mice were used for studies with RH parasites. Each mouse was inoculated via intraperitoneal (i.p) infection with 100 tachyzoites in a 200-μl volume. Plaque assays were performed on a sample of the inoculum to quantify the number of viable tachyzoites in each sample, and only experiments where comparable numbers were obtained were included in our analyses. All animal experiments were conducted with the approval and oversight of the Institutional Animal Care and Use Committee at Stanford University.

Statistics. Statistical analysis was performed with Prism version 6.04 software. For c-Myc, NF-κB, PP2A, p38, and IRF1, comparisons drawn between Δ*myr1* and the wild-type or complemented strains were performed using Student's *t* test. For HMA association, comparison was performed with a chi-square test. For survival curves, comparisons were performed with a log rank Mantel-Cox test.

ACKNOWLEDGMENTS

We thank Chris Tonkin, Justin Boddey, and Michael Coffey (Walter and Eliza Hall Institute of Medical Research) for insightful comments and sharing results prior to publication, Rahul Parulkar (UCSC) for help with the genomic sequencing, Michael Coffey for kindly providing the GRA24-expressing plasmid, Suchita Rastogi for help with the electron microscopy, Stanford Shared FACS facility personnel Bianca Gomez and Tim Knaak for providing technical support during flow cytometry experiments, and the Stanford Neurosciences Microscopy Service for confocal microscopy. We also thank all members of our laboratories for their critical input and useful discussions.

This study was supported by NIH RO1 AI112962 (J.C.B.), NIH T32 AI007328 and the Lawrence Livermore National Lab Institutional Postdoctoral Program (M.F.), NIH P01-35HG000205 (N.P.), NIH T32 AI007290 (M.W.P.), NIH RO1 AI73756 (K.R.B.), NIH F31 AI120649 (N.D.M.), Stanford Graduate Fellowship (N.D.M.), NIH K08AI102946-01 (J.J.B.), Alex's Lemonade Stand Foundation A award (J.J.B.), NIH S10RR025518-01 (Stanford FACS Core), and NIH NS069375 (Stanford Neurosciences Microscopy Services). The funders had no role in study design, data collection and interpretation, or the decision to submit the work for publication.

FUNDING INFORMATION

HHS | National Institutes of Health (NIH) provided funding to John Boothroyd under grant numbers R21-AI112962 and RO1-AI73756. HHS | National Institutes of Health (NIH) provided funding to Magdalena Franco under grant number T32-AI007328. HHS | National Institutes of Health (NIH) provided funding to Nader Pourmand under grant number P01-35HG000205. HHS | National Institutes of Health (NIH) provided funding to Michael William Panas under grant number T32-AI007290. HHS | National Institutes of Health (NIH) provided funding to Nicole D. Marino under grant number F31-AI120649. HHS | National Institutes of Health (NIH) provided funding to Jeffrey J. Bednarski under grant number K08AI102946-01. HHS | National Institutes of Health (NIH) provided funding to Magdalena Franco under grant number S10RR025518-01. HHS | National Institutes of Health (NIH) provided funding to Michael William Panas under grant number P30-NS069375. Alex's Lemonade Stand Foundation for Childhood Cancer (ALSF) provided funding to Jeffrey J. Bednarski.

Stanford University provided the Stanford Graduate Fellowship to Nicole D. Marino.

REFERENCES

1. **Di Cristina M, Marocco D, Galizi R, Proietti C, Spaccapelo R, Crisanti A.** 2008. Temporal and spatial distribution of Toxoplasma gondii differentiation into bradyzoites and tissue cyst formation in vivo. Infect Immun **76:**3491–3501. http://dx.doi.org/10.1128/IAI.00254-08.
2. **Rosowski EE, Saeij JP.** 2012. Toxoplasma gondii clonal strains all inhibit STAT1 transcriptional activity but polymorphic effectors differentially modulate IFNgamma induced gene expression and STAT1 phosphorylation. PLoS One **7:**e51448. http://dx.doi.org/10.1371/journal.pone.0051448.
3. **Yamamoto M, Standley DM, Takashima S, Saiga H, Okuyama M, Kayama H, Kubo E, Ito H, Takaura M, Matsuda T, Soldati-Favre D, Takeda K.** 2009. A single polymorphic amino acid on Toxoplasma gondii kinase ROP16 determines the direct and strain-specific activation of Stat3. J Exp Med **206:**2747–2760. http://dx.doi.org/10.1084/jem.20091703.
4. **Jensen KD, Hu K, Whitmarsh RJ, Hassan MA, Julien L, Lu D, Chen L, Hunter CA, Saeij JP.** 2013. Toxoplasma gondii rhoptry 16 kinase promotes host resistance to oral infection and intestinal inflammation only in the context of the dense granule protein GRA15. Infect Immun **81:**2156–2167. http://dx.doi.org/10.1128/IAI.01185-12.
5. **Ong YC, Reese ML, Boothroyd JC.** 2010. Toxoplasma rhoptry protein 16 (ROP16) subverts host function by direct tyrosine phosphorylation of STAT6. J Biol Chem **285:**28731–28740. http://dx.doi.org/10.1074/jbc.M110.112359.
6. **Rosowski EE, Lu D, Julien L, Rodda L, Gaiser RA, Jensen KD, Saeij JP.** 2011. Strain-specific activation of the NF-kappaB pathway by GRA15, a novel Toxoplasma gondii dense granule protein. J Exp Med **208:**195–212. http://dx.doi.org/10.1084/jem.20100717.
7. **Bougdour A, Durandau E, Brenier-Pinchart MP, Ortet P, Barakat M, Kieffer S, Curt-Varesano A, Curt-Bertini RL, Bastien O, Coute Y, Pelloux H, Hakimi MA.** 2013. Host cell subversion by Toxoplasma GRA16, an exported dense granule protein that targets the host cell nucleus and alters gene expression. Cell Host Microbe **13:**489–500. http://dx.doi.org/10.1016/j.chom.2013.03.002.
8. **Braun L, Brenier-Pinchart MP, Yogavel M, Curt-Varesano A, Curt-Bertini RL, Hussain T, Kieffer-Jaquinod S, Coute Y, Pelloux H, Tardieux I, Sharma A, Belrhali H, Bougdour A, Hakimi MA.** 2013. A Toxoplasma dense granule protein, GRA24, modulates the early immune response to infection by promoting a direct and sustained host p38 MAPK activation. J Exp Med **210:**2071–2086. http://dx.doi.org/10.1084/jem.20130103.

9. **Franco M, Shastri AJ, Boothroyd JC.** 2014. Infection by Toxoplasma gondii specifically induces host c-Myc and the genes this pivotal transcription factor regulates. Eukaryot Cell **13:**483–493. http://dx.doi.org/10.1128/EC.00316-13.
10. **Dang CV, Lewis BC.** 1997. Role of oncogenic transcription factor c-Myc in cell cycle regulation, apoptosis and metabolism. J Biomed Sci **4:**269–278. http://dx.doi.org/10.1007/BF02258350.
11. **Dang CV, Resar LM, Emison E, Kim S, Li Q, Prescott JE, Wonsey D, Zeller K.** 1999. Function of the c-Myc oncogenic transcription factor. Exp Cell Res **253:**63–77. http://dx.doi.org/10.1006/excr.1999.4686.
12. **Blader IJ, Saeij JP.** 2009. Communication between Toxoplasma gondii and its host: impact on parasite growth, development, immune evasion, and virulence. APMIS Acta Pathol Microbiol Immunol Scand **117:**458–476. http://dx.doi.org/10.1111/j.1600-0463.2009.02453.x.
13. **Elsworth B, Matthews K, Nie CQ, Kalanon M, Charnaud SC, Sanders PR, Chisholm SA, Counihan NA, Shaw PJ, Pino P, Chan JA, Azevedo MF, Rogerson SJ, Beeson JG, Crabb BS, Gilson PR, de Koning-Ward TF.** 2014. PTEX is an essential nexus for protein export in malaria parasites. Nature **511:**587–591. http://dx.doi.org/10.1038/nature13555.
14. **Beck JR, Muralidharan V, Oksman A, Goldberg DE.** 2014. PTEX component HSP101 mediates export of diverse malaria effectors into host erythrocytes. Nature **511:**592–595. http://dx.doi.org/10.1038/nature13574.
15. **De Koning-Ward TF, Gilson PR, Boddey JA, Rug M, Smith BJ, Papenfuss AT, Sanders PR, Lundie RJ, Maier AG, Cowman AF, Crabb BS.** 2009. A newly discovered protein export machine in malaria parasites. Nature **459:**945–949. http://dx.doi.org/10.1038/nature08104.
16. **Gold DA, Kaplan AD, Lis A, Bett GC, Rosowski EE, Cirelli KM, Bougdour A, Sidik SM, Beck JR, Lourido S, Egea PF, Bradley PJ, Hakimi MA, Rasmusson RL, Saeij JP.** 2015. The Toxoplasma dense granule proteins GRA17 and GRA23 mediate the movement of small molecules between the host and the parasitophorous vacuole. Cell Host Microbe **17:**642–652. http://dx.doi.org/10.1016/j.chom.2015.04.003.
17. **Garrison E, Treeck M, Ehret E, Butz H, Garbuz T, Oswald BP, Settles M, Boothroyd J, Arrizabalaga G.** 2012. A forward genetic screen reveals that calcium-dependent protein kinase 3 regulates egress in Toxoplasma. PLoS Pathog **8:**e1003049. http://dx.doi.org/10.1371/journal.ppat.1003049.
18. **Hall CI, Reese ML, Weerapana E, Child MA, Bowyer PW, Albrow VE, Haraldsen JD, Phillips MR, Sandoval ED, Ward GE, Cravatt BF, Boothroyd JC, Bogyo M.** 2011. Chemical genetic screen identifies Toxoplasma DJ-1 as a regulator of parasite secretion, attachment, and invasion. Proc Natl Acad Sci U S A **108:**10568–10573. http://dx.doi.org/10.1073/pnas.1105622108.
19. **Coleman BI, Gubbels MJ.** 2012. A genetic screen to isolate Toxoplasma gondii host-cell egress mutants. J Vis Exp **2012:**3807. http://dx.doi.org/10.3791/3807.
20. **Farrell A, Thirugnanam S, Lorestani A, Dvorin JD, Eidell KP, Ferguson DJ, Anderson-White BR, Duraisingh MT, Marth GT, Gubbels MJ.** 2012. A DOC2 protein identified by mutational profiling is essential for apicomplexan parasite exocytosis. Science **335:**218–221. http://dx.doi.org/10.1126/science.1210829.
21. **Zhao B, Zou J, Wang H, Johannsen E, Peng CW, Quackenbush J, Mar JC, Morton CC, Freedman ML, Blacklow SC, Aster JC, Bernstein BE, Kieff E.** 2011. Epstein-Barr virus exploits intrinsic B-lymphocyte transcription programs to achieve immortal cell growth. Proc Natl Acad Sci U S A **108:**14902–14907. http://dx.doi.org/10.1073/pnas.1108892108.
22. **Huang CY, Bredemeyer AL, Walker LM, Bassing CH, Sleckman BP.** 2008. Dynamic regulation of c-Myc proto-oncogene expression during lymphocyte development revealed by a GFP-c-Myc knock-in mouse. Eur J Immunol **38:**342–349. http://dx.doi.org/10.1002/eji.200737972.
23. **Xia D, Sanderson SJ, Jones AR, Prieto JH, Yates JR, Bromley E, Tomley FM, Lal K, Sinden RE, Brunk BP, Roos DS, Wastling JM.** 2008. The proteome of Toxoplasma gondii: integration with the genome provides novel insights into gene expression and annotation. Genome Biol **9:**R116. http://dx.doi.org/10.1186/gb-2008-9-7-r116.
24. **Treeck M, Sanders JL, Elias JE, Boothroyd JC.** 2011. The phosphoproteomes of Plasmodium falciparum and Toxoplasma gondii reveal unusual adaptations within and beyond the parasites' boundaries. Cell Host Microbe **10:**410–419. http://dx.doi.org/10.1016/j.chom.2011.09.004.
25. **Fritz HM, Bowyer PW, Bogyo M, Conrad PA, Boothroyd JC.** 2012. Proteomic analysis of fractionated Toxoplasma oocysts reveals clues to their environmental resistance. PLoS One **7:**e29955. http://dx.doi.org/10.1371/journal.pone.0029955.
26. **Fritz HM, Buchholz KR, Chen X, Durbin-Johnson B, Rocke DM, Conrad PA, Boothroyd JC.** 2012. Transcriptomic analysis of toxoplasma development reveals many novel functions and structures specific to sporozoites and oocysts. PLoS One **7:**e29998. http://dx.doi.org/10.1371/journal.pone.0029998.
27. **Buchholz KR, Fritz HM, Chen X, Durbin-Johnson B, Rocke DM, Ferguson DJ, Conrad PA, Boothroyd JC.** 2011. Identification of tissue cyst wall components by transcriptome analysis of in vivo and in vitro Toxoplasma gondii bradyzoites. Eukaryot Cell **10:**1637–1647. http://dx.doi.org/10.1128/EC.05182-11.
28. **Hiller NL, Bhattacharjee S, van Ooij C, Liolios K, Harrison T, Lopez-Estraño C, Haldar K.** 2004. A host-targeting signal in virulence proteins reveals a secretome in malarial infection. Science **306:**1934–1937. http://dx.doi.org/10.1126/science.1102737.
29. **Marti M, Good RT, Rug M, Knuepfer E, Cowman AF.** 2004. Targeting malaria virulence and remodeling proteins to the host erythrocyte. Science **306:**1930–1933. http://dx.doi.org/10.1126/science.1102452.
30. **Osborne AR, Speicher KD, Tamez PA, Bhattacharjee S, Speicher DW, Haldar K.** 2010. The host targeting motif in exported plasmodium proteins is cleaved in the parasite endoplasmic reticulum. Mol Biochem Parasitol **171:**25–31. http://dx.doi.org/10.1016/j.molbiopara.2010.01.003.
31. **Boddey JA, Hodder AN, Günther S, Gilson PR, Patsiouras H, Kapp EA, Pearce JA, de Koning-Ward TF, Simpson RJ, Crabb BS, Cowman AF.** 2010. An aspartyl protease directs malaria effector proteins to the host cell. Nature **463:**627–631. http://dx.doi.org/10.1038/nature08728.
32. **Russo I, Babbitt S, Muralidharan V, Butler T, Oksman A, Goldberg DE.** 2010. Plasmepsin V licenses Plasmodium proteins for export into the host erythrocyte. Nature **463:**632–636. http://dx.doi.org/10.1038/nature08726.
33. **Coffey MJ, Sleebs BE, Uboldi AD, Garnham AL, Franco M, Marino ND, Panas MW, Ferguson DJ, Enciso M, O'Neill MT, Lopaticki S, Stewart RJ, Dewson G, Smyth GK, Smith BJ, Masters SL, Boothroyd JC, Boddey JA, Tonkin CJ.** 2015. An aspartyl protease defines a novel pathway for export of proteins into the host cell. eLife **4:**e10809.
34. **Mercier C, Adjogble KD, Däubener W, Delauw MF.** 2005. Dense granules: are they key organelles to help understand the parasitophorous vacuole of all Apicomplexa parasites? Int J Parasitol **35:**829–849. http://dx.doi.org/10.1016/j.ijpara.2005.03.011.
35. **Amati B, Littlewood TD, Evan GI, Land H.** 1993. The c-Myc protein induces cell cycle progression and apoptosis through dimerization with Max. EMBO J **12:**5083–5087.
36. **Bretones G, Delgado MD, León J.** 2015. Myc and cell cycle control. Biochim Biophys Acta **1849:**506–516. http://dx.doi.org/10.1016/j.bbagrm.2014.03.013.
37. **Dang CV.** 1999. c-Myc target genes involved in cell growth, apoptosis, and metabolism. Mol Cell Biol **19:**1–11. http://dx.doi.org/10.1128/MCB.19.1.1.
38. **Li Q, Dang CV.** 1999. c-Myc overexpression uncouples DNA replication from mitosis. Mol Cell Biol **19:**5339–5351. http://dx.doi.org/10.1128/MCB.19.8.5339.
39. **Pernas L, Adomako-Ankomah Y, Shastri AJ, Ewald SE, Treeck M, Boyle JP, Boothroyd JC.** 2014. Toxoplasma effector MAF1 mediates recruitment of host mitochondria and impacts the host response. PLoS Biol **12:**e1001845. http://dx.doi.org/10.1371/journal.pbio.1001845.
40. **Kim SK, Fouts AE, Boothroyd JC.** 2007. Toxoplasma gondii dysregulates IFN-gamma-inducible gene expression in human fibroblasts: insights from a genome-wide transcriptional profiling. J Immunol **178:**5154–5165. http://dx.doi.org/10.4049/jimmunol.178.8.5154.
41. **Curt-Varesano A, Braun L, Ranquet C, Hakimi M, Bougdour A.** 13 August 2015. The aspartyl protease TgASP5 mediates the export of the Toxoplasma GRA16 and GRA24 effectors into host cells. Cell Microbiol. http://dx.doi.org/10.1111/cmi.12498.
42. **Hammoudi PM, Jacot D, Mueller C, Di Cristina M, Dogga SK, Marq JB, Romano J, Tosetti N, Dubrot J, Emre Y, Lunghi M, Coppens I, Yamamoto M, Sojka D, Pino P, Soldati-Favre D.** 2015. Fundamental roles of the Golgi-associated Toxoplasma aspartyl protease, ASP5, at the host-parasite interface. PLoS Pathog **11:**e1005211. http://dx.doi.org/10.1371/journal.ppat.1005211.
43. **Minot S, Melo MB, Li F, Lu D, Niedelman W, Levine SS, Saeij JP.** 2012. Admixture and recombination among Toxoplasma gondii lineages ex-

plain global genome diversity. Proc Natl Acad Sci U S A **109:**13458–13463. http://dx.doi.org/10.1073/pnas.1117047109.

44. **Hehl AB, Basso WU, Lippuner C, Ramakrishnan C, Okoniewski M, Walker RA, Grigg ME, Smith NC, Deplazes P**. 2015. Asexual expansion of Toxoplasma gondii merozoites is distinct from tachyzoites and entails expression of non-overlapping gene families to attach, invade, and replicate within feline enterocytes. BMC Genomics **16:**66. http://dx.doi.org/10.1186/s12864-015-1225-x.
45. **Lee PA, Tullman-Ercek D, Georgiou G**. 2006. The bacterial twin-arginine translocation pathway. Annu Rev Microbiol **60:**373–395. http://dx.doi.org/10.1146/annurev.micro.60.080805.142212.
46. **Koshy AA, Fouts AE, Lodoen MB, Alkan O, Blau HM, Boothroyd JC**. 2010. Toxoplasma secreting Cre recombinase for analysis of host-parasite interactions. Nat Methods **7:**307–309. http://dx.doi.org/10.1038/nmeth.1438.
47. **Tobin CM, Knoll LJ**. 2012. A patatin-like protein protects Toxoplasma gondii from degradation in a nitric oxide-dependent manner. Infect Immun **80:**55–61. http://dx.doi.org/10.1128/IAI.05543-11.
48. **Langmead B, Salzberg SL**. 2012. Fast gapped-read alignment with Bowtie 2. Nat Methods **9:**357–359. http://dx.doi.org/10.1038/nmeth.1923.
49. **Gajria B, Bahl A, Brestelli J, Dommer J, Fischer S, Gao X, Heiges M, Iodice J, Kissinger JC, Mackey AJ, Pinney DF, Roos DS, Stoeckert CJ, Jr., Wang H, Brunk BP**. 2008. ToxoDB: an integrated Toxoplasma gondii database resource. Nucleic Acids Res **36:**D553–D556. http://dx.doi.org/10.1093/nar/gkm981.
50. **Radenbaugh AJ, Ma S, Ewing A, Stuart JM, Collisson EA, Zhu J, Haussler D**. 2014. Radia: RNA and DNA integrated analysis for somatic mutation detection. PLoS One **9:**e111516. http://dx.doi.org/10.1371/journal.pone.0111516.
51. **Li H, Handsaker B, Wysoker A, Fennell T, Ruan J, Homer N, Marth G, Abecasis G, Durbin R, 1000 Genome Project Data Processing Subgroup**. 2009. The sequence alignment/map format and SAMtools. Bioinformatics **25:**-2078–2079.
52. **Donald RG, Roos DS**. 1998. Gene knockouts and allelic replacements in Toxoplasma gondii: HXGPRT as a selectable marker for hit-and-run mutagenesis. Mol Biochem Parasitol **91:**295–305. http://dx.doi.org/10.1016/S0166-6851(97)00210-7.
53. **Caffaro CE, Koshy AA, Liu L, Zeiner GM, Hirschberg CB, Boothroyd JC**. 2013. A nucleotide sugar transporter involved in glycosylation of the Toxoplasma tissue cyst wall is required for efficient persistence of bradyzoites. PLoS Pathog **9:**e1003331. http://dx.doi.org/10.1371/journal.ppat.1003331.
54. **Shastri AJ, Marino ND, Franco M, Lodoen MB, Boothroyd JC**. 2014. GRA25 is a novel virulence factor of Toxoplasma gondii and influences the host immune response. Infect Immun **82:**2595–2605. http://dx.doi.org/10.1128/IAI.01339-13.